Middle Jurassic to Early Cretaceous orogenesis in the Klamath Mountains Province (northern California-southern Oregon) occurred by tectonic switching: Insights from Detrital zircon U-Pb geochronology of the Condrey Mountain schist

Alan D. Chapman[1]*

Jennifer Grischuk[2]

Meghan Klapper[3]

William Schmidt[4]

Todd LaMaskin[5]

[1]*Geology Department, Macalester College, Saint Paul, MN 55105, USA*

[2]*Department of Geology and Geophysics, University of Wyoming, Laramie, WY 82071, USA*

[3]*Metropolitan Council of the Twin Cities, Saint Paul, MN 55101, USA*

[4]*Department of Earth Sciences, University of Southern California, Los Angeles, CA 90089, USA*

[5]*Department of Earth and Ocean Sciences, University of North Carolina Wilmington, Wilmington, NC 28403, USA*

This paper is a non-peer reviewed preprint submitted to EarthArXiv.

This paper is under consideration for publication in Geosphere.

Middle Jurassic to Early Cretaceous orogenesis in the Klamath Mountains Province (northern California-southern Oregon) occurred by tectonic switching: Insights from Detrital zircon U-Pb geochronology of the Condrey Mountain schist

Alan D. Chapman[1]*

Jennifer Grischuk[2]

Meghan Klapper[3]

William Schmidt[4]

Todd LaMaskin[5]

[1]*Geology Department, Macalester College, Saint Paul, MN 55105, USA*

[2]*Department of Geology and Geophysics, University of Wyoming, Laramie, WY 82071, USA*

[3]*Metropolitan Council of the Twin Cities, Saint Paul, MN 55101, USA*

[4]*Department of Earth Sciences, University of Southern California, Los Angeles, CA 90089, USA*

[5]*Department of Earth and Ocean Sciences, University of North Carolina Wilmington, Wilmington, NC 28403, USA*

*Email: chapman@macalester.edu

ABSTRACT

The Klamath Mountains province (KMP) of northern California and southern Oregon consists of generally east-dipping terranes assembled via Paleozoic to Mesozoic subduction along the western margin of North America. The KMP more than doubled in mass from Middle Jurassic to Early Cretaceous time, due to alternating episodes of extension (e.g, rifting and formation of the Josephine ophiolite) and shortening (e.g., Siskiyou and Nevadan events). However, the tectonic driving mechanisms surrounding this profound Mesozoic growth of the KMP are poorly understood. In this effort, we show that formation of the Condrey Mountain schist (CMS) of the central KMP spanned this critical time period and use the archive contained within the CMS as a key to deciphering the Mesozoic tectonics of the KMP. Igneous samples from the outer CMS subunit yield U-Pb zircon ages of ca. 175-170 Ma, reflecting the timing of eruption of volcanic protoliths. One detrital sample from the same subunit contains abundant (~54% of analyzed zircon grains) Middle Jurassic ages with Paleozoic and Proterozoic grains comprising the remainder, and yields a maximum depositional age (MDA) of ca. 170 Ma. These ages, in the context of lithologic and thermochronologic relations, suggest that outer CMS protoliths accumulated in an outboard rift basin and subsequently underthrust the KMP during the Late Jurassic Nevadan orogeny. Five samples of the chiefly metasedimentary inner CMS yield MDAs ranging from 160 to 130 Ma, with younger ages corresponding to deeper structural levels. Such inverted age zonation is common in subduction complexes and, considering existing K-Ar ages, suggests that the inner CMS was assembled by progressive underplating over a >10 Myr timespan. Despite this age zonation, age spectra derived from structurally shallow and deep portions of the inner CMS each closely overlap those derived from the oldest section of the Franciscan subduction complex (South Fork Mountain schist). These relations suggest that the inner CMS is a composite of South Fork Mountain schist slices, sequentially underplated beneath the KMP. The age, inboard position, and structural position (i.e. the CMS resides directly beneath Jurassic arc assemblages with no intervening mantle) of the CMS suggests that these rocks were emplaced during one or more previously unrecognized episodes of shallow-angle subduction restricted to the KMP. Furthermore, emplacement of the deepest portions of the CMS corresponds with the ca. 136 Ma termination of magmatism in the KMP, which we relate to disruption of asthenospheric flow during slab shallowing. The timing of shallow-angle subduction shortly precedes that of the westward translation of the KMP relative to correlative rocks in the northern Sierra Nevada Range, suggesting that subduction dynamics were responsible for relocating the KMP from the arc to the forearc. In aggregate, the above relations require at least three distinct phases of extension and/or rifting, each followed by an episode of shallow-angle underthrusting. The dynamic upper plate deformation envisioned here is best interpreted in the context of tectonic switching, whereby slab steepening and trench retreat alternates with slab shallowing due to recurrent subduction of buoyant oceanic features.

Keywords: Tectonic switching, Siskiyou orogeny, Nevadan orogeny, tectonic underplating, slab rollback, shallow-angle subduction, Klamath Mountains Province, Condrey Mountain schist, detrital zircon geochronology

1. INTRODUCTION

Upper plate domains of subduction zones are sites of significant arc magmatism, terrane accretion, tectonic underplating, tectonic erosion, delamination, and (possibly) relamination (e.g., Bird, 1979; Von Huene and Lallemand, 1990; Davies and Stevenson, 1992; Stern and Scholl, 2010; Scholl and von Huene, 2009; Hacker et al., 2011; Jacobson et al., 2011). Mass flux calculations involving these processes indicate that, compared with other tectonic settings, subduction zones are the biggest producers and destroyers of continental lithosphere on the planet (Cloos and Shreve, 1988; Kay and Kay, 1991; Von Huene and Scholl, 1991; Gutscher et al., 2000; Arndt, 2013).

Material fluxes to and from the overriding plate of a subduction zone are influenced by changes in dip angle of the downgoing plate (Coney and Reynolds, 1977; Dewey, 1981; Collins, 2002; Brun and Faccenna, 2008; Schellart and Strak, 2021). For instance, sufficient shallowing of slab dip tends to inhibit arc magmatism via impingement of mantle wedge corner flow, while promoting tectonic erosion through an increase in shear stress along the base of the upper plate (e.g., Saleeby, 2003). Furthermore, upper plate shortening leads to mountain building and an increase in erosion; the resulting flood of detritus to the trench may drive significant accretion and/or tectonic underplating (e.g., Ducea et al., 2009). Conversely, steepening of a slab from a shallow trajectory (i.e., “slab rollback”) may (re)ignite arc magmatism and lead to upper plate extension and migration of the trench oceanward (e.g., Chapman et al., 2021). In particular, switching from shallow- to steep-angle subduction and vice versa appears to be an efficient net producer of continental crust (Collins, 2002).

In detail, upper plate domains of modern subduction zones respond to changes in downgoing slab dip in diverse ways. For instance, magmatism in the Trans-Mexican Volcanic Belt has continued in spite of flat subduction of the Cocos plate beneath it, most likely due to slab melting plus nascent slab rollback and associated influx of new asthenosphere (e.g., Ferrari et al., 2012). Furthermore, sufficient decoupling may result in a lower plate that glides into the mantle at low dip with minimal upper plate deformation, as appears to be the case along the Mexican flat slab (Pérez-Campos et al., 2008).

Recognition of ancient settings in which subduction trajectory varied is essential to understanding modern counterparts, as the geologic record permits investigation of the long-term (i.e., millions to tens of millions of years) effects of changes in slab dip over a range of crustal depths. The Pelona-Orocopia-Rand (and related) schists of southern California represent an excellent example of such an archive of ancient slab shallowing followed by steepening (Grove et al., 2003; Jacobson et al., 2011; Chapman, 2017).

The Klamath Mountains Province of northern California – southern Oregon apparently underwent rapid alternation between contraction and extension, most notably from Middle Jurassic to Early Cretaceous time (Saleeby et al., 1982; Harper and Wright, 1984; Wright and Wyld, 1986; Wright and Fahan, 1988; Hacker and Ernst, 1993; Harper et al., 1994; Hacker et al., 1995; Harper, 2003; Snoke and Barnes, 2006; Yule et al., 2006; LaMaskin et al., 2022; Surpless et al., 2023). Tectonic activity coincided with significant magmatic additions to the plate margin (Harper, 1984; Barnes et al., 1996; Allen and Barnes, 2006; Snoke and Barnes, 2006; Coint et al., 2013; Barnes and Barnes, 2020). The driving mechanisms behind tectonism and magmatism in the KMP are controversial, with competing ideas ranging from global plate reorganization to collision of a large fragment of continental lithosphere (Schweickert and Cowan, 1975; Wernicke and Klepacki, 1988; Wright and Fahan, 1988; May et al., 1989; McClelland et al., 1992; Saleeby and Harper, 1993; Hacker et al., 1995; Wolf and Saleeby, 1995; Shervais et al., 2004; Seton et al., 2012; LaMaskin et al., 2022; Surpless et al., 2023). Both mechanisms predict extensive deformation over extended periods, yet observed contractional and extensional episodes were seemingly confined to a few hundred kilometers along the margin and occurred rapidly (in many cases, within less than 10 million years and often less than 5 million years). This paper contributes new U-Pb igneous and detrital zircon data from the Condrey Mountain schist, a unit of unknown origin exposed within a structural window in the central KMP, as it provides key constraints on the Middle Jurassic to Early Cretaceous tectonic evolution of the KMP. With new time constraints in hand, we reassess the mechanisms driving orogenesis, the formation of ophiolite-floored basins, and magmatism in the KMP in the context of rapid changes in slab dip. These new data greatly facilitate regional correlation of the Condrey Mountain schist, a longstanding regional geologic problem.

2. GEOLOGIC BACKGROUND

2.1. Paleozoic and Mesozoic assembly of the Klamath Mountains Province

Numerous long (100s to 1000s of km), parallel, arcuate belts of accreted material comprise the North American Cordillera, resulting from hundreds of millions of years of convergent margin tectonics following Neoproterozoic rifting of supercontinent Rodinia and the development of an "Atlantic-type" passive margin (Burchfiel et. al., 1992; Dickinson, 2004; Blakey and Ranney, 2018). Here, we focus on Paleozoic and Mesozoic events germane to construction of the Klamath Mountains Province and adjacent Franciscan assemblages (Fig. 1).

Neoproterozoic to Devonian basement rocks of the Eastern Klamath terrane, interpreted as dismembered remnants of island arcs of the Paleo-Pacific (i.e., Panthalassa) ocean, are the cornerstone of the Klamath Mountains upon which the remainder of the range was built (Moores, 1970; Speed, 1979; Burchfiel et al., 1992; Wallin and Metcalf, 1998; Wallin et al., 2000; Wright and Wyld, 2006; Grove et al., 2008; Fig. 1). Prior to docking with the western margin of North America, in Silurian-Devonian time, oceanic assemblages of the Central Metamorphic terrane underplated the Eastern Klamath terrane along an east-dipping subduction zone (Davis, 1968; Irwin, 2003; Barrow and Metcalf, 2006). The resulting composite terrane was conveyed toward, and collided with, the western margin of North America via a west-dipping subduction zone, driving Late Permian-Early Triassic closure of the Golconda-Slide Mountain basin and eastward thrusting of deep-water assemblages atop shallow water passive margin sequences in the Great Basin and adjacent areas (i.e., the Sonoma orogeny; Speed, 1977; Wyld, 1991; Burchfiel et al., 1992; Dickinson, 2000). Incorporation of the Eastern Klamath and Central Metamorphic terranes with the North American plate was accompanied by formation of the Fort Jones/Stuart Fork accretionary complex, the along-strike equivalent of the Cache Creek assemblage of the Canadian Cordillera (e.g., Johnston and Borel, 2007, and arc magmatism (the "McCloud arc" of

Miller, 1987) above the eastward subducting Panthalassa lithosphere (Wright, 1982; Coleman et al., 1988; Goodge, 1989).

The Paleozoic-Early Mesozoic nucleus of the Klamath mountains (i.e., the three terranes discussed above) grew significantly during the Middle Jurassic (ca. 170 Ma) Siskiyou orogeny (Coleman et al., 1988; Wright and Fahan, 1988; Hacker et al., 1995; Snoke and Barnes, 2006; Barnes et al., 2006). This event involved sequential accretion of three additional "terranes." The first and most easterly of which is the Sawyers Bar terrane, formerly divided into North Fork, Salmon River, and Eastern Hayfork subterranes, together representing a Permian oceanic arc, overlying Permian-Triassic deep sea and terrigenous sedimentary cover, plus outboard accretionary wedge (Coleman et al., 1988; Ernst, 1990; Hacker et al., 1993, 1995; Scherer and Ernst, 2008; Scherer et al., 2010; Ernst et al., 2017). Accretion of the Western Hayfork terrane, a ca. 177-167 Ma continent-fringing oceanic arc (Harper and Wright, 1984; Wright and Fahan, 1988; Barnes and Barnes, 2020), and its dismembered ophiolitic basement (the Rattlesnake Creek terrane) followed (Wright and Fahan, 1988; Donato et al., 1996). In detail, the Rattlesnake Creek terrane consists of basal serpentinite matrix mélange, overlying comagmatic ca. 193-207 Ma mafic volcanic plus plutonic assemblages, and volcaniclastic and hemipelagic cover strata, locally overprinted by amphibolite-granulite facies parageneses (Irwin, 1972; Wright, 1982; Coleman et al., 1988; Wright and Wyld, 1994; LaMaskin et al., 2021).

The Rattlesnake Creek terrane is nonconformably overlain by pre-164 Ma greenschist facies mafic intrusive and volcanic rocks plus hemipelagic sedimentary rocks (the Preston Peak complex; e.g., Snoke, 1977; Saleeby et al., 1982) and tectonically underlain by ca. 172-170 Ma amphibolite facies mafic volcanic rocks and hemipelagic sediments (the China Peak complex; Saleeby and Harper, 1993). Both China Peak and Preston Peak complexes are interpreted as early products of extension that culminated in the ca. 164-162 Ma Josephine ophiolite, the basement of the Western Klamath terrane (Saleeby and Harper, 1993). Lithologic and age similarities between the China Peak and Preston Peak complexes suggest that the former may represent the underthrust equivalent of the latter (Saleeby and Harper, 1993).

The Siskiyou event was immediately followed by rifting of newly accreted Rattlesnake Creek-Western Hayfork crust, forming the ca. 164-162 Ma Josephine ophiolite-floored basin. Rifting is envisioned to have occurred at a high-angle to the margin in a transtensional regime, such that the locus of spreading separated the active arc into the ca. 165-156 Ma Wooley Creek plutonic belt in the south and the ca. 161-155 Ma Rogue-Chetco arc in the north (Saleeby et al., 1982; Harper, 1984; Wright and Wyld, 1986; Wright and Fahan, 1988; Hacker and Ernst, 1993; Harper et al., 1994; Harper, 2003; Snoke and Barnes, 2006; Yule et al., 2006; Coint et al., 2013). For this reason, the Josephine basin has been deemed a site of ancient "interarc" rifting. This is misleading, however, as an "interarc rift" conjures images of parallel arcs separated by a rift. More accurately, rifting likely occurred in the forearc outboard of the Wooley Creek plutonic belt in the south (e.g., Harper, 2003), traversed the arc, and occurred in the retroarc inboard of the Rogue-Chetco arc in the north.

Deposition of the Galice Formation ensued in the submarine Josephine marginal basin, first with ca. 162-157 Ma (Oxfordian) argillite and transitioning to ca. 160-150 Ma (Oxfordian-Kimmeridgian) turbidite, as regional extensional stresses yielded to contractile deformation associated with the ca. 157-150 Ma Nevadan orogeny (Saleeby and Harper, 1993; Harper et al., 1994; Schweickert et al., 1984; Hacker et al., 1995; Miller and Saleeby, 1995; Shervais et al., 2004; MacDonald et al., 2006; Gradstein et al., 2020; LaMaskin et al., 2021; Surpless et al., 2023). The Nevadan event is responsible for thrusting the Western Klamath terrane (including the Rogue-Chetco arc plus consanguineous Josephine ophiolite and nonconformably overlying Galice formation) beneath previously accreted materials. There is no consensus at this time regarding the driving mechanism(s) for Nevadan and Siskiyou events. End-member models invoke either collisions of oceanic ridges or far-traveled lithospheric blocks such as the Wrangellia-Alexander superterrane (e.g., Schweickert and Cowan, 1975; Wernicke and Klepacki, 1988; McClelland et al., 1992; Saleeby and Harper, 1993; Shervais et al., 2004; Surpless et al., 2023) and/or changes in relative plate motion (e.g., Wright and Fahan, 1988; Wolf and Saleeby, 1995; Hacker et al., 1995; LaMaskin et al., 2021).

In Early Cretaceous time, the Klamath Mountains Province relocated ~200 km westward to achieve its current forearc position and concave-east arcuate curvature relative to correlative rocks in the northern Sierra Nevada and Blue Mountains (Fig. 1 inset; Jones and Irwin, 1971; Ernst, 2013). Following this episode, 1) magmatism in the Klamaths abruptly terminated ca. 136 Ma, in marked contrast to the Sierra Nevada and Blue Mountains where magmatism continued until Late Cretaceous time (Chen and Moore, 1982; Lund and Snee. 1988; Barnes et al., 1996;

Allen and Barnes, 2006); 2) an accretionary wedge, represented by the eastern belt of the Franciscan Complex, formed and grew rapidly along the western edge of the Western Klamath terrane (Dumitru et al., 2010); 3) the Western Klamath terrane, eastern belt Franciscan rocks, and the Condrey Mountain schist (discussed in the following section) cooled from ~400 to ~200 ˚C between ca. 135 and 118 Ma (Helper, 1985; Harper et al., 1994; Batt et al., 2010a; Dumitru et al., 2010; Tewksbury-Christle et al., 2021); 4) low-angle normal faulting commenced in the eastern Klamaths (Cashman and Elder, 2002; Batt et al., 2010b); and 5) topography built up during earlier tectonism was lost during an eastward sweeping Valanginian-Hauterivian marine transgression across the majority of the Klamath Mountains province (Harper et al., 1994; Batt et al., 2010a). The significance of these relations and a discussion of possible driving mechanisms are explored in section 5.4.

2.2. Condrey Mountain schist

The Condrey Mountain schist (CMS) stands out as an unusual feature of the KMP. The unit is exposed as a domal structural window through the overlying Rattlesnake Creek terrane, beneath the low-angle Condrey Mountain shear zone (Mortimer and Coleman, 1985; Fig. 2). This structural arrangement significantly differs from the usual westward-younging stack of east-dipping thrust sheets observed in the KMP. Furthermore, the CMS resides at lower metamorphic grade and yields younger cooling ages relative to flanking rocks (Helper 1985; Hacker et al., 1995; Tewksbury-Christle et al., 2021). Efforts to fit the CMS into the regional puzzle have focused on lithologic and age similarities with adjacent rocks, resulting in correlations with the Central Metamorphic terrane (Irwin, 1960); Stuart Fork terrane (Medaris, 1966), the Galice Formation (Klein, 1977; Hotz, 1979; Saleeby and Harper, 1993), the China Peak complex (Saleeby and Harper, 1993), and the South Fork Mountain schist (the oldest Franciscan unit of significant areal size; Suppe and Armstrong, 1972; Brown and Blake, 1987). The Central Metamorphic and Stuart fork terranes are now known to be significantly older than the CMS, rendering earlier correlations untenable (Hotz et al., 1977).

The CMS is subdivided into a structurally deeper, relatively low-grade inner unit and structurally higher, relatively high-grade marginal unit, separated by the Condrey Internal fault (Helper, 1986; Saleeby and Harper, 1993; Figs. 1 and 2). Both CMS subunits preserve similar prograde ductile non-coaxial deformation and texturally late coaxial flattening fabrics, attributed to subduction-related burial and later structural ascent, respectively (Helper, 1986).

The inner CMS consists chiefly of greenschist to blueschist grade graphitic and quartz-mica schist, likely produced through metamorphism of argillite and chert protoliths, that locally contain lenses and tabular slabs of blueschist (formerly basaltic flows and tuff) and serpentinite (Hotz, 1979; Helper, 1986; Saleeby and Harper, 1993; Tewksbury-Christle et al., 2021). The array of rock types observed within the inner CMS, and the paucity of clastic material therein, point to sedimentation in an open ocean starved of terrigenous input atop a basement and/or including olistoliths of oceanic lithosphere.

The outer CMS mantles the inner unit and includes greenschist to amphibolite facies metamorphosed basaltic tuffs, pillow lavas, and rare comagmatic intrusive equivalents and plagiogranite. These igneous protoliths dominate the outer CMS though are locally interrupted by lenses of hemipelagic material (now silicic and graphitic quartz-mica schist) and one prominent (~10 km-long x 0.5 km wide in map view) semi-pelitic horizon exhibiting graded beds, likely representing deep-water turbidite deposits (Hotz, 1979; Helper, 1985). The range of lithologies observed in the outer CMS suggest oceanic deposition proximal to an eruptive center with sporadic input of terrigenous material.

Along the “Scott River appendage,” the outer CMS reaches amphibolite facies as the Condrey Mountain shear zone is approached from below (Saleeby and Harper, 1993; Figs. 2 and 3). Metamorphic grade also increases down-section within the Rattlesnake Creek terrane, preserving upper amphibolite and locally granulite facies parageneses, as the Condrey Mountain shear zone is approached from above (Hotz, 1979; Mortimer and Coleman, 1985; Garlick et al., 2009). These relations require a sharp inverted metamorphic field gradient spanning structurally deep, low-grade inner CMS and higher-grade outer CMS.

3. METHODS

3.1. U-Pb Geochronology

Ten samples were collected for U-Pb zircon analysis. These include: 1) three samples from the outer CMS (two from a plagiogranite inclusion transposed into the main foliation of surrounding actinolite schist previously investigated by Saleeby and Harper [1993], and one from the semi-pelite of Helper [1985]); 2) five samples from the inner unit (three from the "Dry Lake" area of Helper [1985], the deepest exposed level of the CMS, and two from structurally higher); 3) one sample from the Gold Flat amphibolite [Burton, 1982] of uncertain affinity (either representing the base of the Rattlesnake Creek terrane or the top of the outer CMS); and 4) one sample of uncertain origin from a structurally complex zone ~5 km east of Happy Camp (representing hemipelagic protoliths of either the Galice formation or CMS). Coordinates are provided for all sampled localities in Table 1.

Zircon grains were extracted using standard mineral separation techniques of crushing, sieving, magnetic separation, processing through heavy liquids, and hand picking. Separates were then mounted in epoxy, polished, and imaged on the Macalester Keck Lab JEOL 6610 LV Scanning Electron Microscope (SEM) before analysis.

U-Pb geochronology of igneous and detrital zircon was conducted by laser ablation multicollector inductively coupled mass spectrometry (LA-MC-ICPMS) at the Arizona LaserChron Center (ALC) following the methods outlined in Gehrels et al. (2006). Zircon grains were ablated using a 193 nm ArF laser with a pit depth of ~12 μm and spot diameters of 35 μm for sample 14CM21 and 20 μm for all other samples. Fragments of in-house Sri Lanka (SL) and Forest Center (Duluth Complex; FC-1) zircon standards, respectively with isotope dilution–thermal ionization mass spectrometry (ID-TIMS) ages of 563.5 ± 3.2 Ma and 1099 ± 0.6 Ma (2σ), were analyzed once per every five unknown analyses to correct for instrument mass fractionation (Paces and Miller, 1993; Gehrels et al., 2008). A secondary standard R33 (Black et al., 2004) with ID-TIMS age of 418.9 ± 0.4 Ma (2σ) was analyzed once per every fifty unknown analyses. A weighted mean 206Pb/238U age of 420.4 ± 3.5 Ma (2σ, mean square of weighted deviates [MSWD] = 0.22) was calculated from a total of 29 analyses of R33 performed at the ALC. Data reduction was done using in-house ALC Microsoft Excel programs and ISOPLOT/Ex Version 3 (Ludwig, 2003). This process included calculation for average intensity, correcting for background interference, calculating isotopic ratios and ages. Analyses with greater than 10% uncertainty, 20% discordance, and/or 5% reverse discordance were excluded.

Normalized, cumulative probability, and multi-dimensional scaling plots were constructed with detritalPy (Sharman et al., 2018) using 207Pb/206Pb ages for grains older than 900 Ma and 206Pb/238U ages for grains younger than 900 Ma.

Detrital geochronology provides constraints on the maximum depositional ages (MDAs) of (meta)sedimentary rocks, though a wide range of techniques exist for calculating MDAs (e.g., Dickinson and Gehrels, 2009; Sharman et al., 2018; Coutts et al., 2019; Vermeesch, 2021). Methods based on the youngest single grain (YSG), the youngest clusters of grains, and TuffZirc or AgePick algorithms – were avoided as they drift to younger ages with increasing number of analyses (Vermeesch, 2021). Similarly, estimates based on the weighted mean or mode of the youngest peak of a probability density plot were not used due to underlying issues of probability density plots (Vermeesch, 2012). We present MDAs in Table 2 calculated via youngest statistical population (YSP; Coutts et al., 2019) and maximum likelihood algorithm (MLA; Vermeesch, 2021) techniques, as these methods are least likely to yield ages younger than the true depositional age. The "interpreted age" column in Table 2 factors in MDA calculations and regional thermochronologic data, if available.

4. RESULTS

4.1. Petrography and Metamorphic Petrology

Samples 14CM16, 15KM11, 15KM14, 19KM4, and 19KM5, were all collected from the internal metasedimentary CMS unit. Of these, samples 14CM16, 19KM4, and 19KM5 are from the Dry Lake area of Helper (1986), the deepest exposed portion of the CMS. At this location, these hemipelagic protoliths are recumbently folded with metamorphosed mafic volcanic assemblages that equilibrated at pressure-temperature conditions of 380-450 ˚C and 6-11 kbar (Helper, 1986; Tewksbury-Christle et al., 2021; Fig. 4a). Additional constraints are placed on the P-T trajectory of metamorphism in the CMS through thermodynamic modeling. The Gibbs free energy minimization software package THERIAK-DOMINO (de Capitani and Brown, 1987) and the thermodynamic end-member and solution models of the accompanying 'tc321p2' database

(THERMOCALC database as distributed in version 3.33) were used to construct P-T pseudosections in the NCKFMASH system.

Dry Lake metasedimentary rocks contain chiefly medium- to fine-grained quartz, albitic plagioclase, phengitic to paragonitic white mica, carbonaceous material, and chlorite, which locally exhibits pseudomorphs after pyrite up to 1 cm in diameter. Minor phases include epidote, zoisite, titanite, and stilpnomelane. Thermodynamic modeling, using bulk compositions reported by Hotz (1979), shows this mineral paragenesis to be stable at the conditions reported above for metavolcanic units, corroborating the assertion that metavolcanic and metasedimentary assemblages at Dry Lake represent metamorphosed relict stratigraphy (Helper, 1986; Fig. 5). These samples exhibit well-developed flattening fabrics containing tight to isoclinal and disharmonic folds best expressed by intervals rich in white mica and carbonaceous material (Fig. 4b).

Samples 15KM14 and 15KM11 were collected from the structural top of the inner CMS in the vicinity of White Mountain, < 1 km from the Condrey Mountain Internal Fault, and exhibit mylonitic foliation characterized by spaced white (quartz plus albite) and pale- to medium green (chlorite, white mica, and carbonaceous material) domains with local preservation of tight isoclinal folds (Fig. 4c). Pyrite pseudomorphs similar to those at the Dry Lake area were observed in the outcrop from which sample 15KM14 was extracted. Notably, these samples lack epidote group minerals, suggesting that peak metamorphic temperatures in the vicinity of White Mountain were ~100˚C higher, at similar pressure, than those achieved in the Dry Lake area (Fig. 5).

The bulk of the outer CMS consists of albitic plagioclase, actinolite, chlorite, epidote, and white mica with minor quartz and titanite, consistent with equilibration of these metavolcanic assemblages under greenschist facies conditions (Fig. 5). Sample 15KM23 is from a semi-pelitic interval in the otherwise metabasaltic marginal unit of the CMS (Fig. 2; Helper, 1985, 1986). This sample exhibits alternating highly cleaved chlorite- plus carbonaceous material- rich domains and microlithons containing subequal proportions of quartz and chlorite (Fig. 4d). Plagioclase is apparently lacking from this sample and epidote is observed as a minor phase throughout the sample and appears to have statically overgrown earlier formed cleaved and microlithon domains.

Sample 14CM21, collected from the Gold Flat amphibolite of either the uppermost CMS or lowermost Rattlesnake Creek terrane, is a coarse blastomylonitic amphibolite gneiss containing chiefly pargasitic amphibole, anorthitic plagioclase, and epidote, with minor apatite and ilmenite, and rare coarse (~1 cm) garnet porphyroblasts (Fig. 4e and 4f). The Gold Flat amphibolite equilibrated at peak metamorphic conditions of 630 ± 50 ˚C at 7.3 ± 1.0 kbar, corresponding to transitional albite-epidote amphibolite/upper amphibolite conditions (Klapper and Chapman, 2017) and overlapping the H2O-saturated solidus for outer CMS metabasite (Fig. 5).

Samples 14CM17 and 15KM49 were collected from a coarse-grained felsic interval displaying a foliation concordant with that of encasing outer CMS actinolite schist. These relations point to an intrusive protolith that invaded the outer CMS prior to underthrusting and metamorphism. These samples are dominated by quartz and albitic plagioclase with subsidiary white mica, biotite, chlorite, and pyrite (Fig 4g).

The NE margin of a reentrant of Western Klamath terrane assemblages paralleling the Klamath River (the "Klamath River Appendage" of Saleeby and Harper, 1993) is of uncertain affinity. While most maps show assign exposed greenschist facies hemipelagic rocks to the Galice Formation, Hill (1984) interprets these rocks as a <5 km-wide window of inner CMS lying structurally above the Galice Formation and beneath the China Peak complex. Sample 19KM3 was collected from this window with the aim of clarifying the affinity of these rocks (Fig. 2). This sample contains a greenschist facies assemblage of quartz, chlorite, white mica, carbonaceous material, and minor epidote, arranged in tightly folded quartz-rich and micaceous domains (Fig. 4h).

4.2. Zircon U-Pb Geochronology

Results from U-Pb zircon analysis of the CMS and samples of unknown affinity are reported below, summarized in Table DR1, and illustrated in Figures 6 and 7.

4.2.1. CMS Igneous Analysis

15KM49 and 14CM17: These samples of meta-plagiogranite yielded 46 and 107 concordant U-Pb zircon ages, respectively, from which a concordia age of 171.8 ± 0.8 (2σ) was calculated (Fig. 6). This age is identical within uncertainty to a 172 ± 2 Ma age reported by Saleeby and Harper (1993) from a ~100 m-scale gneissic metadiorite sill collected <5 km from the studied locality.

4.2.2. CMS Detrital Analyses

15KM23: This sample is from the western portion of the marginal CMS unit and is the structurally highest metasedimentary sample studied here. Concordant ages from 135 zircon grains range from 161.4 ± 4.8 to 2898.3 ± 12.0 Ma (1σ; Fig. 7). The sample yields YSP and MLA MDAs of 169.5 ± 0.6 and 170.8 ± 0.7 Ma (1σ), respectively. It should be noted that these values are based on a large cluster of ~50 ages that overlap at the 1σ level and is probably too conservative. The majority of analyzed grains (54%) yield Jurassic ages, with the most pronounced peak centered at 168 Ma. Paleozoic populations (21% of the total) exhibit minor peaks occurring at 268, 320, 329, 390 and 486 Ma. “Timanian/Pan-African-age” (i.e., 540-700 Ma) grains make up 5% of the total. Proterozoic populations include a broad swath of “Grenville-age” (i.e., 950-1300 Ma) grains (7%) plus distinct peaks at 1350 Ma, 1500 Ma and 1630 Ma, corresponding to 5%, 3% and 5% of analyzed grains, respectively. Four isolated Archean grains range from 2500 to 2900 Ma.

15KM14: MDAs of 159.8 ± 1.6 Ma (1σ) were calculated from this sample (YSP and MLA methods produce identical results), which yielded 90 concordant U-Pb zircon ages ranging from 156.5 ± 3.9 Ma to 2484.1 ± 24.9 Ma (1σ). This sample is characterized by a spiky distribution of U-Pb ages, with peaks at ca. 160, 410, 1020, 530, and 620 Ma. Jurassic, Paleozoic, Timanian/Pan-African, and Grenville-age components comprise 10%, 30%, 11%, and 24% of the total, respectively. Scattered Proterozoic grains with ages >1100 Ma plus one ca. 2750 Ma grain make up 28% of analyzed grains.

15KM11: This sample yielded 119 concordant U-Pb zircon ages suitable for provenance analysis and the largest disparity between calculated MDAs (YSP: 144.5 ± 1.5 Ma; MLA: 153.4 ± 1.1 Ma; 1σ). Analyzed grains range in age from 141.1 ± 2.5 to 2958.2 ± 20 Ma (1σ). In this sample, 24.3% of the grains are Jurassic, exhibiting a distinct peak at ca. 158 Ma and auxiliary peak at ca.

190 Ma. Paleozoic ages comprise 18% of the total and exhibit numerous minor age peaks at ca. 275, 325, and 365-440 Ma. A distinct population of Timanian/Pan-African-ages (8%) with a peak at ca. 610 Ma, Grenville-age grains (16%), and less prominent peaks at ca. 1450, 1500, and 1680 comprise the bulk of remaining ages. This sample also yielded three ca. 2000 Ma and two 2900 Ma ages.

14CM16: This sample was collected from the summit of Condrey Mountain at the northern edge of the Dry Lake area (Helper, 1986), the deepest exposed portion of the Condrey Mountain structural window. The 73 concordant U-Pb zircon ages calculated from this sample range from 131.7 ± 3.9 to 2078.2 ± 44.3 Ma (1σ) and yield MDAs of 139.5 ± 1.9 and 142.5 ± 2.4 Ma (1σ), by YSP and MLA methods, respectively. As in other samples analyzed from the CMS, the largest peak in terms of area is Jurassic (22% of the total), with a peak falling at ca. 160 Ma. Auxiliary early Mesozoic age peaks are observed at ca. 225 and 250 Ma. Paleozoic populations (15% of the total) concentrate at ca. 340, 430, and 510 Ma. A population of Timanian/Pan-African ages makes up 16% of analyzed grains and exhibits a conspicuous ca. 600 Ma peak. Grenville-age grains exhibit a peak at ca. 1030 Ma and account for 19% of the sample. Scattered Proterozoic ages with one low relief peak at 1450 Ma make up most of the remaining ages.

19KM5: This sample was collected 2 km SE of sample 14CM16, within the Dry Lake area, and yielded 274 U-Pb ages suitable for provenance analysis. These ages span 129.5 ± 4.3 to 3295.4 ± 12.1 Ma (1σ) and yield YSP and MLA MDAs of 135.1 ± 0.9 and 135.5 ± 1.0 Ma (1σ), respectively. In order of decreasing prominence, the age peaks exhibited by this sample are: ca. 158 Ma (with a broad Jurassic shoulder comprising 18% of total grains), 240 Ma, Grenville-age grains (26%) with peaks at 1020 and 1150 Ma, Paleozoic ages (15%) with a 390 Ma peak, and Timanian/Pan-African populations (7%) at ca. 550 Ma and 610 Ma. Pre-Grenville-age grains are generally scattered with discernable peaks at ca. 1440, 1660, and 1910 Ma, with an array of Neoarchean ages.

19KM4: This sample was collected 1 km SE of the previous sample, again from the Dry Lake area, and yielded 284 concordant U-Pb ages ranging from 128.2 ± 2.2 to 2862.6 ± 10.3 Ma (1σ). Respectively, YSP and MLA MDAs of 130.7 ± 0.9 and 130.2 ± 1.7 Ma (1σ) were calculated from this sample. Jurassic, Paleozoic, Timanide/Pan-African-age, and Grenville-age populations comprise 14%, 23%, 14%, and 19% of the total, respectively. This sample exhibits three sharp

Phanerozoic peaks of diminishing prominence at 158, 260, and 400 Ma plus another prominent Neoproterozoic peak at 600 Ma. Broader subsidiary peaks, ordered by decreasing amplitude, occur at ca. 1060, 1440, 1200, 1660, 2110, and 2710 Ma.

4.2.3. Samples of Unknown Affinity

14CM21: This sample of sheared migmatitic gneiss of the Gold Flat amphibolite of either the upper portion of the outer CMS or the deepest portion of the Rattlesnake Creek terrane yielded a unimodal ca. 167 to 209 Ma spread of ages from 14 CL-dark, oscillatory-zoned zircon core domains, from which a concordia age of 171.1 ± 1.6 Ma (2σ) was determined. Thin (<20 μm), CL-bright domains exist on nearly all analyzed grains; two analyses of such domains yielded relatively high-U/Th ratios (~5-7) and ages of 150.0 ± 2.1 and 163.8 ± 3.3 Ma. The textures and geochemistry observed in zircon rims suggest that these domains are of metamorphic origin, though insufficient ages were determined to calculate the timing of recrystallization.

19KM3: Respectively, YSP and MLA MDAs of 162.1 ± 0.4 Ma and 164.2 ± 0.4 Ma (1σ) were calculated from this sample, which yielded 184 concordant U-Pb zircon ages ranging from 150.6 ± 12.2 Ma to 2747.3 ± 13.4 Ma (1σ). This sample exhibits a dominant peak at ca. 166 Ma, with Jurassic grains making up 48% of the total, and an auxiliary peak at ca. 260 Ma. Scattered Paleozoic (12%) peaks concentrated at ca. 350 and 450 Ma, Grenville-age grains (6%) with a peak at ca. 950 Ma, and pre-Grenville-age grains with peaks at 1480 and 1780 Ma comprise most remaining grains. Timanian/Pan-African grains are rare in this sample, making up only 3%.

5. DISCUSSION

In this section, we 1) address local geologic problems pertaining to the affinities of the Gold Flat amphibolite and schist exposed at the NE margin of the Klamath River appendage; 2) infer the ages and sources of the CMS to evaluate possible regional correlations; 3) discuss the mechanisms that likely controlled assembly of the CMS, and 4) provide a model for emplacement of the CMS in the context of Mesozoic plate motions.

5.1.1. Affinity of the Gold Flat Amphibolite

The Gold Flat amphibolite was assigned by Barrows (1969) and Burton (1982) to the base of the Rattlesnake Creek terrane, in the upper plate of the Condrey Mountain shear zone, on the basis of structural position and the presence of garnet-bearing amphibolite facies assemblages. However, it is conceivable that the Gold Flat amphibolite represents the amphibolite facies culmination of a documented north-to-south field metamorphic gradient, beginning in greenschist facies outer CMS assemblages near the confluence of the Scott and Klamath rivers (Barrows, 1969; Saleeby and Harper, 1993). Indeed, our U-Pb data from oscillatory zoned zircon core domains from the Gold Flat amphibolite point to igneous crystallization of this unit ca. 171 Ma (Fig. 6), ~20 Myr younger than the youngest dated igneous protoliths from the Rattlesnake Creek terrane (c.f., Wright and Wyld, 1994) and overlapping ages from igneous protoliths of the outer CMS. The "Scott River granophyre" of Saleeby and Harper (1993), a relatively large leucosome sampled from the Gold Flat amphibolite, yielded a slightly discordant multi-fraction age of 157 +3/-2 Ma, which these workers attributed to some combination of inheritance plus open system behavior. New results from single zircon crystals extracted from the same leucosome material yield U-Pb ages of 155.3±0.3 Ma (Gates et al., 2019). We interpret the array of ages determined from the Gold Flat amphibolite to reflect mixing of igneous and metamorphic grain domains. The above lithologic and geochronologic relations strongly suggest that the Gold Flat unit does not belong to the Rattlesnake Creek terrane, in the upper plate of the Condrey Mountain shear zone, and instead represents migmatitic amphibolite facies equivalents to the outer CMS. Alternatively, the Gold Flat amphibolite may represent an exposure of ca. 170 Ma intrusive material, such as the Vesa Bluffs pluton or Ironside Mountain batholith, that sporadically intrude the Rattlesnake Creek terrane.

5.1.2. Affinity of the NE Klamath River Appendage

Accurate regional tectonic models depend critically on the correct identification of rocks exposed along the NE margin of the Klamath River appendage (Figs. 1 and 2). The assertion of Hill (1984) that the inner CMS intervenes between the Galice Formation and China Peak complex has significant implications for: 1) the relative age of the CMS (deposited and buried first), Galice Formation (deposited after), and Nevadan orogeny (during which the Galice

Formation underthrust the CMS) and 2) the magnitude of slip along Nevadan structures (e.g., the Orleans fault) responsible for Galice burial.

Sample 19KM3 yields a Late Jurassic MDA and shows significant age spectrum overlap with both the Galice Formation (LaMaskin et al., 2021; Surpless et al., 2023) and, to a lesser degree, the lens of semipelite within the outer CMS (sample 15KM23, this study; Figs. 7, 8, and 9; Table 2). These samples are all characterized by significant populations of Jurassic ages (~half of analyzed grains) and Paleoproterozoic and older ages, with low proportions of Paleozoic plus Timanian/Pan-African- and Grenville-age grains. The age spectra and MDAs derived from the inner CMS do not match those of sample 19KM3 as closely.

Hence, detrital zircon ages in sample 19KM3 are most compatible with a Klamath River appendage Galice and/or an outer CMS metasedimentary origin. The paleogeographic/tectonic scenario that led to similarities in detrital zircon age spectra between the Galice Formation of the Klamath River assemblage, outer CMS metasediments, and sample 19KM3 will be explored further in the sections that follow.

5.2. Age and provenance of the Condrey Mountain schist

5.2.1. Outer Condrey Mountain Schist

Igneous samples from the outer CMS yield U-Pb ages of ca. 171-170 Ma (Saleeby and Harper, 1993; this work; Fig. 6), which we interpret to reflect the timing of eruption and emplacement of mafic volcanic and intrusive protoliths. One detrital sample (15KM23), recovered from the "semipelite" interval of Helper (1985) in the center of the outer CMS, yields an MDA of ca. 170 Ma. Given the approximately unimodal Middle-to-Late Jurassic age peak derived from this sample, we infer that its hemipelagic protolith was sourced largely from the adjacent ca. 170 Ma Western Hayfork arc and possibly consanguinous China Peak complex (additional discussion of this relationship below), with input of pre-Jurassic grains from the eastern KMP or further inboard.

The outer CMS shares a similar range of lithologies (e.g. metamorphosed mafic volcanic and intrusive rocks and subordinate metasedimentary rocks and felsic dikes), an overlapping range of igneous ages, and an identical structural position (beneath the Rattlesnake Creek terrane along a regional thrust fault) with the China Peak complex. Alternatively, the Western Hayfork terrane may represent a suitable correlative to the outer CMS, given that each consist of ca. 170 Ma volcaniclastic strata and tuffaceous intervals of basaltic to andesitic composition. However, the China Peak complex and Western Hayfork terrane may be consanguineous, and distinguishing between them is therefore futile. However, we consider a Western Hayfork terrane -outer CMS link less likely given that the Western Hayfork terrane resides structurally above the Rattlesnake Creek terrane (e.g., Donato, 1987; Saleeby and Harper, 1993; Barnes and Barnes, 2020).

Correlation of the outer CMS with underthrust China Peak assemblages leads us to infer the following paleogeographic setting for the formation of the outer CMS unit, adapted from Donato (1987) and Saleeby and Harper (1993).

At ca. 175 Ma (a few Myr prior to formation of outer CMS protoliths), the Klamath Mountains Province consisted of four terranes inboard of the Rattlesnake Creek terrane, upon which the Western Hayfork arc was being constructed. The arrangement of this framework plus the high-Mg andesite and adakite geochemistry of the Western Hayfork terrane likely reflects eastward subduction of young, hot Farallon oceanic lithosphere (Barnes and Barnes, 2020). At ca. 172 Ma, a phase of extension affected this framework, perhaps due to some combination of: 1) a rapid change in the absolute motion of North America (May and Butler, 1986; Saleeby and Harper, 1993) and 2) upper-lower plate coupling above an aging, and cooling, subducting Farallon plate (i.e., slab rollback). Extensional tectonism localized within the Western Hayfork and Rattlesnake Creek terranes, forming sheeted dikes of the China Peak and Preston Peak complexes and covering the region with volcaniclastic to hemipelagic sediment. Rifting was interrupted by the ca. 170 Ma Siskiyou event, leading to regional shortening and thrusting of the Western Hayfork terrane >15 km beneath the Sawyers Bar terrane, followed by minor thrusting of the Rattlesnake Creek terrane beneath the Western Hayfork terrane, and stitching of these terranes by batholith-scale intrusives (Wright, 1982; Wright and Fahan, 1988; Barnes and Barnes, 2020). At ca. 164 Ma, shortening waned and extension resumed, generating the Josephine ophiolite and hemipelagic precursors to the Galice Formation, while the Rogue-Chetco and Wooley Creek volcano-plutonic belts flanked the Josephine basin.

Following rifting and formation of the Josephine basin, extension yielded to shortening once again with the ca. 157 Ma onset of the Nevadan event. Cooling ages from the outer CMS and the base of the Rattlesnake Creek terrane strongly suggest that these units were juxtaposed at this time (Helper, 1985; Saleeby and Harper, 1993; Hacker et al., 1995). The presence of China Peak protoliths within the Condrey Mountain window requires at least 50 km of underthrusting along the Condrey Mountain shear zone. This shear zone juxtaposes the outer CMS with the exposed rootless base of the Wooley Creek plutonic belt and its Rattlesnake Creek terrane framework. Removal of the base of the Wooley Creek belt and emplacement of the outer CMS with no intervening mantle strongly suggests that shearing must have occurred at an anomalously low-angle. We suggest that the heat required for greenschist to upper amphibolite facies metamorphism in the outer CMS and outboard equivalents in the China Peak complex was supplied from the upper plate, which had been recently invaded by the 165-156 Ma Wooley Creek plutonic belt.

5.2.2. Inner Condrey Mountain Schist: Provenance

Metasedimentary rocks in the inner CMS, including both White Mountain and Dry Lake subunits, are lithologically similar and yield overlapping distributions of detrital zircon grains from structurally deep to shallow levels. All analyzed samples from the inner CMS exhibit a prominent Middle to Late Jurassic age peak, centered at ca. 160 Ma. This Jurassic population was most likely sourced from ca. 165-156 Ma plutons and ca. 156-152 Ma late-stage intrusives of the Wooley Creek belt (Hacker et al., 1995; Irwin and Wooden, 1999; Snoke and Barnes, 2006; MacDonald et al., 2006; Coint et al., 2013), with probable input from the ca. 161-155 Ma Rogue-Chetco arc and/or plagiogranite derived from underlying Josephine ophiolite basement (Harper et al., 1994). Additional contributions from eroded Jurassic plutons of the Sierra Nevada arc and retroarc are also likely, as Hf isotopic analysis of Middle-Late Jurassic grains extracted from the Galice Formation require an origin outside of the KMP (Surpless et al., 2023).

The majority of detrital zircon grains contained within the inner CMS are pre-Mesozoic, some of which (e.g., Paleoproterozoic and older grains) may be explained through westward shedding of material eroded from the Siskiyou and/or Nevadan orogenic highlands to the east (Figs. 8 and 9). However, it should be noted that the inner CMS contains higher proportions of Grenville-age and Permian-Triassic detrital zircon grains and lower proportions of Paleoproterozoic grains than observed in pre-CMS assemblages of the Klamaths, such as the Fort Jones/Stuart Fork and Sawyers Bar terranes (Sherer and Ernst, 2008; Scherer et al., 2010; Ernst, 2017). Furthermore, the inner CMS contains distinct Paleozoic and Timanian/Pan-African-age peaks, centered at 400 and 600 Ma, respectively.

These relations require inmixing of at least one additional source component containing abundant Grenville-age, Permian-Triassic, Paleozoic, and Timanian/Pan-African-age detrital zircon grains. Recycled Triassic backarc basin strata of Nevada and eastern California (Manuzak et al., 2000; Darby et al., 2000; Gehrels and Pecha, 2014; Dickinson and Gehrels, 2008; LaMaskin et al., 2011) and/or Jurassic erg materials of the Colorado Plateau and adjacent areas (e.g., Dickinson and Gehrels, 2003, 2009) are excellent candidates for the extraregional input(s) required to fully explain detrital zircon age spectra of the inner CMS. Incorporation of one or both of these components likely involved erosion in the backarc region, perhaps within the Luning-Fencemaker thrust belt (e.g., Wyld, 2002; Wyld et al., 2003) or the Mogollon Highlands (Mauel et al., 2011), and westward routing of resulting detritus along the flanks of the elevated Klamath-northern Sierra Nevada before entering the Josephine basin. This recycled backarc signal observed in the inner CMS is likewise noted in clastic materials of the Franciscan Eastern belt, the Galice Formation, and the basal Great Valley Group. This detrital component was, therefore, ubiquitous within the Late Jurassic-Early Cretaceous forearc realm, and strongly suggests the arc was not yet prominent enough to block detritus from the continental interior (DeGraaf-Surpless et al., 2002; Surpless et al., 2006; Dumitru et al., 2010; Orme and Surpless, 2019; LaMaskin et al., 2021; Surpless et al., 2023; Schmidt and Chapman, in prep; Figs. 8 and 9)

Early Cretaceous detrital zircon grains are found only at deep structural levels of the inner CMS. These grains most likely originated from some combination of two sources: 1) ca. 142 to 136 Ma plutons of tonalitic to granodioritic composition (Snoke and Barnes, 2006) exposed throughout the Klamaths and/or 2) volcanic ash erupted from the ca. 130-140 Ma westernmost edge of the Sierran arc, now largely buried beneath Great Valley forearc basin strata (Saleeby, 2007). An airfall origin for ca. 137 Ma and younger zircon in the South Fork Mountain schist is inferred by Dumitru et al. (2010) based on the abundance of very small grains of these ages in radiolarian chert, a rock type not known for incorporation of significant clastic material.

Some models for the Jurassic to Cretaceous tectonic evolution of the KMP call on collision of the southern flank of the Wrangellia-Alexander composite terrane (e.g., Tipper, 1984; Wernicke and Klepacki, 1988; McClelland et al., 1992). This model predicts some detrital contributions from the Wrangellia-Alexander terrane to sediment being deposited in intervening basins (e.g., the Galice Formation, the SFMS, and the CMS) during its approach. Recent detrital zircon geochronology from late Paleozoic strata of the southern Wrangellia-Alexander terrane, exposed on Vancouver Island (British Columbia, Canada), reveals abundant Carboniferous ages (ca. 344-317 Ma) and very few pre-400 Ma grains (Alberts et al., 2021). This Carboniferous component is not recognized in the Galice formation, SFMS, or CMS, suggesting either that Paleozoic strata of the Wrangellia-Alexander terrane were not exposed during collision, that Wrangellia-Alexander terrane-derived sediment was not shed toward the KMP, or that the terrane did not collide at the paleolatitude of the Klamath Mountains in the Jurassic to Cretaceous time frame.

5.2.3. Inner Condrey Mountain Schist: Age

Structurally shallow samples (i.e., subjacent to the Condrey Internal fault and in the vicinity of White Mountain; Fig. 2) yield older MDAs compared with those from the Dry Lake area (ca. 160-153 Ma versus ca. 143-130 Ma; Table 2, Fig. 10). It is conceivable that the entire inner CMS pile was deposited synchronously and that the local environment in which structurally shallow samples were deposited did not receive significant quantities of Early Cretaceous detrital zircon. We consider this unlikely since K-Ar white mica ages vary from ca. 141 Ma beneath the Condrey Internal fault to ca. 128 Ma in the Dry Lake area (Lanphere et al., 1968; Helper, 1985). These age relations suggest that the outermost portion of the inner CMS was buried, grew metamorphic white mica, and cooled through K-Ar closure prior to deposition of Dry Lake area protoliths. We suggest that samples directly beneath the Condrey Internal fault represent a package of material distinct from that observed at deeper structural levels. In reality, the inner CMS is likely composed of more than two tectonic slices, as noted by Tewksbury-Christle et al. (2021), though sheared boundaries separating packages have not been directly observed, perhaps due to poor exposure or because they are gradational. Coupling Ar-Ar thermochronology with detrital zircon U-Pb geochronology would provide a means of resolving additional slices, if present. Regardless, regional correlation of the inner CMS and its subunits has significant implications for the late Mesozoic tectonic development of the Klamath Mountains Province.

5.2.4. The Inner CMS: Galice or Franciscan?

The protoliths of the inner CMS, lower hemipelagic section of the Galice Formation, and the South Fork Mountain schist (hereafter SFMS) each consist chiefly of argillite and chert and therefore do not facilitate regional correlation. However, the abundance of turbidite in the upper portion of the Galice Formation and its absence from the CMS window render correlation of these units unlikely.

The structurally deep Dry Lake area contains the youngest material of the CMS. Detrital zircon age spectra and Early Cretaceous MDAs calculated from this area overlap those from the SFMS (Dumitru et al., 2010; Chapman et al., 2021b; Schmidt and Chapman, in preparation). This observation, in addition to structural and lithologic similarities between these units, strongly suggest that this portion of the CMS represents Franciscan assemblages displaced ~100 km inboard from the nearest previously recognized exposures of South Fork Mountain schist.

The structurally shallow White Mountain area yields MDAs older than structurally deep samples and overlapping those reported for the Galice Formation (LaMaskin et al., 2021; Surpless et al., 2023). However, the detrital zircon age spectra of White Mountain subunit samples more closely overlaps those of the Dry Lake subunit and SFMS compared to the Galice Formation. For these reasons, we consider a White Mountain CMS-Galice correlation unlikely.

It is conceivable that sedimentary protoliths in the White Mountain Area were deposited synchronously with those in the Dry Lake area, with the former not receiving detrital zircons of Early Cretaceous age. Indeed, Tewksbury-Christle et al. (in review) document a minute quantity (<1%) of Early Cretaceous detrital zircon grains within the White Mountain subunit.

Alternatively, the White Mountain area may represent a slice of pre-SFMS Franciscan, perhaps the Skaggs Springs schist. The Skaggs Springs schist of the Franciscan eastern belt represents a possible precursor to the much more voluminous, yet comparable metamorphic grade, South Fork Mountain schist (Dumitru et al., 2010). Compared to the South Fork Mountain schist, the Skaggs Springs schist yields an older maximum depositional age (ca. 144 Ma) and a younger main age peak (ca. 152 versus 162 Ma; Snow et al., 2010). It is important to note, however, that these differences are based on a small number (38) of analyses available from the Skaggs Springs schist, rendering the relationships between the inner CMS and these important Franciscan units uncertain.

It could be argued that the inner CMS is not equivalent to the SFMS, as the former yields older (141-128 Ma; Helper, 1985) white mica K-Ar ages compared to Ar-Ar ages from the latter (ca. 123 Ma; Dumitru et al., 2010). However, this difference may result from limited data (three or fewer samples from both units) and/or the indirect comparability of datasets (K-Ar versus Ar-Ar).

It is also possible that the CMS represents SFMS protoliths that subducted a few Myr earlier than the remainder of the SFMS. Our favored interpretation, explored in the sections that follow, is that the CMS was emplaced during a phase of shallow-angle subduction with limited strike-parallel extent. Such an episode could conceivably result in localized CMS subduction prior to regional SFMS emplacement. Furthermore, the presence of Franciscan assemblages in the Condrey Mountain window, and likely continuing at least ~50 km east of the window (observed as a ~3 km-thick low velocity layer; Fuis et al., 1987), requires significant low-angle underthrusting of subduction accretion assemblages.

5.3. Middle to Late Jurassic Tectonic Evolution of the Klamath Mountains Province and Emplacement of the Outer Condrey Mountain Schist

The CMS appears to be a composite of three distinct units. First, emplacement of the outer CMS subunit, inferred to be greenschist to amphibolite grade equivalents of the China Peak complex, beneath the Rattlesnake Creek terrane most likely occurred during the Nevadan event. Next, a section of probable eastern Franciscan belt equivalents (White Mountain subunit) underthrust the outer CMS after ca. 153-144 Ma (Table 1), possibly in the waning stages of the Nevadan event. Assembly of the CMS culminated with tectonic underplating of the innermost Dry Lake CMS subunit of Franciscan affinity, constrained to the interval between ca. 140 Ma maximum depositional ages and ca. 128 Ma K-Ar cooling ages. We explore the tectonic implications of this apparent three-stage emplacement history of the CMS below.

Regional tectonism was clearly very dynamic preceding and attending underthrusting of the outer and White Mountain subunits of the CMS, involving rapid changes from extension and formation of the China Peak complex, to shortening (Siskiyou phase), followed again by extension (Josephine basin-formation), and culminating with convergence (burial of the outer CMS, Western Klamath terrane, and the White Mountain unit of the inner CMS). It is important to note that the change from ca. 170 Ma Siskiyou convergence to ca. 164 Ma Josephine extension to ca. 157 Ma Nevadan convergence over a brief time interval has long been recognized (e.g., Wright and Fahan, 1988; Hacker and Ernst, 1993; Snoke and Barnes, 2006). However, current models for the Jurassic tectonic development of the Klamath Mountains Province face challenges in explaining the swift transitions between periods of contraction and extension, as well as the spatial restriction of deformation.

The driver(s) of Siskiyou and Nevadan events are unclear, with debate surrounding the relative roles of changes in plate motion versus the collision of exotic lithosphere, namely the Wrangellia-Alexander superterrane. Changes in the rate and/or orientation of convergence between western North America and the Panthalassan realm ca. 170 Ma and 150 Ma (e.g., May et al., 1989; Seton et al., 2012) have be invoked to explain Siskiyou and Nevadan deformation. If a global plate reorganization did indeed occur, why was deformation localized to a <500 km-long domain of the margin? Should the Siskiyou and/or Nevadan events have not lasted longer? Should these events not have been bracketed and interrupted by similarly brief and localized extensional episodes? Similar challenges arise with collisional models, as modern (e.g. the Alpine and Himalayan) and ancient (e.g., the Grenville, Appalachian-Caledonian, and Laramide) examples span 1000s of km and several 10s of Myr. Furthermore, recent U-Pb detrital zircon geochronology from Rattlesnake Creek and Western Klamath terranes strongly suggests a western North America-fringing origin for these terranes, ruling out the possibility that they represent far-travelled materials such as the Wrangellia-Alexander superterrane (LaMaskin et al., 2021).

In light of the above issues with models invoking changes in plate motion or superterrane collision, we suggest that rapidly alternating periods of localized extension and shortening are better understood in the context of "tectonic switching" (Collins, 2002). In this context, the Siskiyou event was preceded by a brief ca. 172 Ma extensional episode, as evidenced by sheeted dike complexes of the Preston Peak and China Peak complexes and the diverse array of magmas (Barnes and Barnes, 2020) generated in the Western Hayfork (extensional?) arc. Extensional tectonism may have been related to slab retreat and/or oceanward stepping of subduction (e.g., Donato, 1987). The Siskiyou event occurred ca. 170 Ma with docking of fringing Rattlesnake Creek and Western Hayfork terranes. Encroachment of these terranes with earlier accreted materials was most likely accomplished by subduction of a small (less than a few 100 km in diameter) yet buoyant and rough oceanic feature (e.g. a plateau, aseismic ridge, seamount chain, or fracture zone) embedded in subducting Panthalassa lithosphere, thereby enhancing basal traction along the subduction interface. Subduction of relatively smooth and thin oceanic lithosphere followed shortly after passage of this hypothetical oceanic feature; ensuing slab retreat induced an ~5 Myr phase of upper plate extension and forming the Josephine basin. Relatively steep subduction enabled asthenospheric counterflow and devolatilization melting, leading to magmatism in the Wooley Creek plutonic belt and Rogue-Chetco arc. At ca. 157 Ma (the Nevadan event), upper plate magmatism waned and extension yielded to shortening due to subduction of another buoyant and rough oceanic feature, underthrusting the outer CMS and the Western Klamath terrane. The punctuated and localized effects of impingement of multiple small oceanic features with the Middle-Late Jurassic margin of North America at the paleolatitude of the Klamath Mountains finds analogs in modern rough patches of subducting oceanic lithosphere, such as the Australian and Philippine Sea plates (LaMaskin et al., 2011; Lallemand et al., 2018). Alternatively, buckling of the downgoing slab along mantle density interfaces may have played an additional role (e.g., Schellart and Strak, 2021).

In summary, the Jurassic evolution of the Klamath Mountains Province exhibits the hallmark traits of a region that has experienced tectonic switching, namely localized and rapidly alternating contraction and extension. An argument could be made, though, that the rough patches of seafloor crucial for tectonic switching were subducted into the mantle, rendering the model untestable. However, a fragment of the Middle Jurassic seafloor is preserved in the Rattlesnake Creek terrane. The existence of dismembered ophiolitic mélange in the Rattlesnake Creek terrane strongly suggests that the seafloor being conveyed toward the North American margin was a highly irregular surface.

5.4. Shallow-Angle Subduction Model for Early Cretaceous Assembly of the Inner Condrey Mountain Schist, Franciscan Accretion, and Klamath-Sierran Separation

Magmatism resumed as deformation associated with the Nevadan orogeny waned, permitting intrusion of primarily mafic magmas belonging to the ca. 151-144 Ma western Klamath suite (Barnes et al., 2006). Following intrusion of the western Klamath suite, the locus of magmatism migrated a modest amount (a few 10s of km) eastward and evolved toward more felsic compositions (ca. 142-136 Ma tonalite-trondhjemite-granodiorite and granodioritic suites; Barnes et al., 1992). Magmatism in the KMP abruptly terminated ca. 136 Ma (Allen and Barnes, 2006).

We infer the above relations to have resulted sequentially from: 1) post-Nevadan slab rollback and associated extensional magmatism within the opening mantle wedge; 2) slab shallowing and related arc migration plus incorporation of previously subcreted materials (e.g., Allen and Barnes, 2006); and 3) shallow/flat subduction, impingement and/or removal of the circulating mantle wedge, and arc shutdown. Shortly after the cessation of magmatism, several additional noteworthy events occurred in the KMP (Figs. 10 and 11).

First, the continental margin transitioned from non-accretion to an accretionary mode marked by the emplacement of the oldest slices of Franciscan (i.e., the SFMS) beneath the KMP along the Coast Range fault (Dumitru et al., 2010; Chapman et al., 2021b). These authors argue, based on observations from modern forearcs (e.g. Clift and Vannucchi, 2004; Scholl and von Huene, 2007), that accretion began in response to an increase in sedimentary flux into the trench. They conclude that the driving mechanism(s) behind increased sedimentation is(are) unclear, though may relate to an increase in magmatic flux in the Sierra Nevada batholith, erosion of orogenic highlands, and/or changes in relative plate motion.

It is difficult to envision the localized (i.e., KMP-adjacent) increase in sedimentation required for Franciscan and inner CMS accretion as being driven by regional- (i.e., Sierra Nevada-scale) to global-scale phenomena. Instead, we speculate that localized (no more than a few 100s of km along orogenic strike) shallow-angle subduction led to increased basal traction along the margin, leading to growth of the accretionary wedge and an increase in underplating. Correlation of the inner CMS Dry Lake subunit with the SFMS requires that the former accumulated in the Early Cretaceous trench and underthrust the KMP along the equivalent of the Coast Range fault. The shallowly-dipping tectonic contact separating KMP basement and lower plate inner CMS requires tectonic erosion of formerly intervening mantle lithosphere.

Second, the KMP relocated westward from the axis of arc magmatism to the forearc domain and was affected by extension (Constenius et al., 2000; Batt et al., 2010a, 2010b; Ernst, 2013). Ernst (2013) invokes a decrease in upper-lower plate coupling to explain these relations, speculating that a change in subducting material from old (i.e., cold and thick) to young (i.e., warm and thin) oceanic lithosphere may be responsible. We concur that extension and westward motion of the KMP likely involved a reduction of interplate coupling. However, subduction of a <200 km-wide patch of a young oceanic lithosphere flanked by significantly older lithosphere finds no modern analogs, except where spreading ridges are colliding with continental margins; if a spreading center had collided with the KMP in Early Cretaceous time, evidence for an elevated geothermal gradient at that time should be present. Instead, we suggest that slab rollback from the originally shallower trajectory profoundly reduced upper-lower plate coupling, facilitating trench retreat, westward displacement of the KMP, and extension within the province.

The proposed Early Cretaceous shallow-angle subduction episode and ensuing rollback mark the final events of more than 50 Myr of tectonic switching experienced by the KMP. To summarize, two pronounced cycles of tectonic switching include: 1) ca. 175-170 Ma extension, during which the China Peak complex, Western Hayfork arc, and outer CMS protoliths formed followed by the ca. 170 Ma Siskiyou event and 2) ca. 164-162 Ma extension and formation of the Josephine basin followed by the ca. 157-151 Ma Nevadan event. A relatively feeble third event is marked by ca. 151-144 Ma formation of western Klamath suite magmas, slab shallowing and inboard migration of magmatism, and ca. 140-128 Ma shallow-flat slab emplacement of the Dry Lake subunit of the inner CMS. A final phase of extension, and associated deep marine sedimentation, in the KMP accompanied its westward translation in the ca. 136-125 Ma window (Ernst, 2013).

5.5. What is Franciscan and what portions of the Condrey Mountain Schist qualify?

Hallmarks of the Franciscan Complex, summarized by Berkland et al. (1972) and Wakabayashi (2015) include: 1) the presence of diverse lithologies, consisting chiefly of metamorphosed clastic sedimentary rocks with lesser amounts of serpentinite, basalt, chert, and limestone; 2) metamorphism along a high-pressure/low temperature array, generally spanning the zeolite, prehnite-pumpellyite, blueschist, and eclogite facies; 3) depositional and metamorphic ages spanning Early Cretaceous to Paleogene time; 4) residing structurally beneath Middle to Late Jurassic ultramafic rocks, gabbro, and basalt of the Josephine ophiolite in northern California/southern Oregon and the Coast Range ophiolite in more southerly California; and 5) displaying a variety of structural styles from generally coherent to internally broken to mélange.

The Dry Lake subunit meets all criteria listed above, contains a similar array of rock types to the South Fork Mountain schist, and MDAs and detrital zircon age spectra from the South Fork Mountain schist and Dry Lake subunit overlap significantly. The White Mountain subunit is likewise lithologically identical to the South Fork Mountain Schist and Dry Lake subunit. However, despite hosting detrital zircon grains yielding a similar array of ages to the South Fork Mountain Schist and Dry Lake subunit, the White Mountain subunit yields older MDAs. Age constraints on the emplacement of this subunit are virtually absent, with small quantities of Early Cretaceous detrital zircon grains (Tewksbury-Christle et al., in review) and a single white mica K-Ar age of ca. 144 Ma reported (Lanphere et al., 1968), raising the possibility that this subunit indeed accreted in Early Cretaceous time. Is the White Mountain subunit of the inner CMS Franciscan? The only apparent reason to exclude the subunit appears to be on the basis of its age. For this reason, we recommend that the White Mountain subunit of the inner CMS be considered Franciscan.

Reimagining the entire inner CMS as Franciscan has implications for what controlled accretion of clastic units in the Franciscan, as the inner CMS may represent the oldest known slice of predominantly sedimentary material contained in the Franciscan. If, as we suggest, emplacement of the inner CMS was controlled by one or more episodes of shallow-angle subduction, then the switch from non-accretion to accretion (e.g. Dumitru et al., 2010) may have been flipped as the slab shallowed.

Is the outer CMS Franciscan? This unit contains chiefly basaltic flows and pyroclastic deposits metamorphosed under greenschist to amphibolite facies conditions in Middle to Late Jurassic time, at odds with the Franciscan characteristics listed above. Furthermore, the structural relationship between the outer CMS and the Josephine ophiolite is unclear, as the outer CMS probably represents the buried equivalents of early rift products. If the outer CMS does indeed represent a buried early rift facies of the Josephine ophiolite, then protoliths of the outer CMS were likely emplaced in and erupted onto marginal North American crust, notably distinct from the trench setting in which the Franciscan Complex formed. These relations lead us to suggest that the outer CMS does not belong to the Franciscan Complex. However, burial of the ophiolitic upper plate to the Franciscan appears to be restricted to the outer CMS and broadly correlative Josephine ophiolite of the KMP, as the Coast Range ophiolite of more southerly California did not experience burial-related metamorphism exceeding zeolite grade (Evarts and Schiffman 1983). Such burial and accretion of the outer CMS, while distinct in character from the Franciscan, marked the end of a protracted phase of non-accretion and heralded the arrival of the first packages of Franciscan assemblages.

5.6. A comparison with the Pelona-Orocopia-Rand and related schists of southern California and Arizona

The Late Cretaceous-early Cenozoic Pelona-Orocopia-Rand (POR) and related schists of southern California and Arizona represent the world's best-known example of the exhumed products of shallow-angle subduction (e.g., Saleeby, 2003; Jacobson et al., 2007; Chapman, 2017). Five key observations, summarized by Ducea et al. (2009) and Chapman (2017), reveal the tectonic significance of the POR schist. First, the schist consists chiefly of continent-derived immature clastic material with subordinate oceanic rocks – typical subduction-accretion assemblages – residing beneath continental arc plutons of the continental interior. Second, the contact between these rock packages is a shallow-angle ductile structure separating lower plate schist and upper plate arc assemblages. Third, the lower plate exhibits an inverted metamorphic field gradient and achieves peak temperatures ~100 ˚C lower than the overriding plate. Fourth, the depositional and metamorphic ages of lower plate clastic materials broadly overlap with the intrusive ages of upper plate plutons, requiring underthrusting at plate tectonic rates. Finally, outside of the schist outcrop belt the arc is separated from subduction accretion assemblages (i.e. the Franciscan Complex to the north and Western Baja terrane to the south) by a forearc basin underlain by ophiolitic basement and sub-continental mantle lithosphere. In other words, the lateral extent of shallow-angle subduction-related damage is apparently restricted to the schist domain where forearc lithosphere is absent.

Saleeby (2003) argue based on observed margin-parallel tectonostratigraphic variations that Late Cretaceous subduction along the western margin of North America consisted of normally-dipping domains interrupted by a shallowly-dipping segment in southern California.

This argument was later bolstered by forward and inverse geodynamic modeling strongly suggesting that a conjugate to the Shatsky Rise of the NW Pacific Ocean basin collided with southern California in Late Cretaceous time (Liu et al., 2010).

The CMS satisfies all shallow-angle subduction criteria, with one caveat. Like the POR schist, the CMS contains chert plus mafic and ultramafic rocks of oceanic origin. However, the POR schist and CMS are dominated by psammitic and hemipelagic protoliths, respectively. This key difference reflects deposition of POR schist protoliths proximal to the continent, probably along the trench slope, whereas CMS protoliths probably represent more distal trench-floor deposits. Some combination of the following factors probably led to this key lithologic difference: a higher sedimentation and/or plate convergence rate for the case of the POR schists or the presence of basement highs or lows that blocked coarse clastic material from becoming part of the CMS section (e.g., Underwood et al., 1980; Engebretsen et al., 1984).

One additional hallmark of shallow-angle subduction, noted by Coney and Reynolds (1977) in the SW North American Cordillera, is a migrating locus of magmatism that sweeps inboard during slab shallowing. For the case of the KMP, the relative positions of Latest Jurassic and Early Cretaceous plutons implies relatively modest arc migration within this time frame (a few 10s of km; Snoke and Barnes, 2006). However, the entire KMP moved off the axis of magmatism in Early Cretaceous time, separating from the Sierran arc, to reside ~200 km to the west in the forearc realm (e.g., Ernst, 2013). Therefore, if magmatism at the latitude of the KMP indeed continued from Early into middle Cretaceous time, then the products of said magmatism would be expected east of the KMP. Unfortunately, basement rocks east of the KMP are covered by several km of sedimentary and volcanic rocks, including the Upper Cretaceous Hornbrook Formation, Paleogene volcaniclastic rocks of the Payne Cliffs and Colestin formations, and Plio-Quaternary volcanic rocks of the Cascade Range and Modoc Plateau provinces (Berge and Stauber, 1987; Fuis et al., 1987; Guffanti et al., 1996). To our knowledge, no basement derived xeno-liths/-crysts are reported from the area separating the KMP and the Basin and Range. Though direct constraints are lacking, seismic data suggest that southern Cascade Range and Modoc Plateau crust are likely underlain by igneous and metamorphic rocks related to the KMP and northern Sierra Nevada (e.g., Fuis et al., 1987).

6. CONCLUSIONS

The purpose of this effort is to constrain the origin of the CMS. To that end, new zircon U-Pb geochronology from the outer CMS unit points to ca. 171 Ma eruption of volcanic protoliths and deposition of infolded nonconformably overlying metasedimentary rocks shortly thereafter. Outer CMS sedimentary protoliths comprise chiefly KMP-derived detritus. The greenschist-to-amphibolite grade inverted metamorphic field gradient preserved in the outer CMS is inferred to have formed during ca. 156-152 Ma (i.e. Nevadan) underthrusting of the unit directly beneath the ca. 167-156 Ma (i.e., recently extinguished at that time and hence, hot) Wooley Creek plutonic belt. In aggregate, the outer CMS appears to represent products of early-stage Josephine basin rifting, akin to similar "rift edge facies" assemblages such as the China Peak and Preston Peak complexes, that underthust the Middle-Late Jurassic arc and its Rattlesnake Creek terrane framework during the Nevadan orogeny.

The inner CMS is petrogenetically distinct from the outer CMS, to the degree that referring to each as portions of the same unit may no longer be practical. Detrital zircon U-Pb ages derived from the inner CMS reveal a downsection decrease in calculated MDAs from ca. 160 Ma adjacent to the Condrey Internal fault to ca. 130 Ma at the deepest level of exposure. This observation, integrated with sparse K-Ar white mica age constraints, leads us to subdivide the inner CMS into structurally high and low White Mountain and Dry Lake subunits, respectively. Based on similar rock types and comparable detrital zircon age spectra, we correlate both subunits of the inner CMS with the eastern belt of the Franciscan Complex.

Tectonic underplating of the White Mountain subunit beneath previously emplaced outer CMS must pre-date arrival of the Dry Lake subunit, to explain their older-on-younger structural arrangement (the former yields MDAs >10 Myr older than the latter). The precise timing of underthrusting of each unit is unclear. However, we suspect that the White Mountain subunit was emplaced during the waning stages of the Nevadan event. Arrival of the Dry Lake subunit must postdate calculated MDAs spanning 143-130 Ma and possibly occurred ca. 128 Ma, the K-Ar age of metamorphic white mica derived from this subunit.

These results suggest that the CMS represents forearc-trench assemblages emplaced beneath the Late Jurassic arc in at least three distinct pulses. The first two occurred in rapid succession, with underplating of the outer CMS and White Mountain subunit of the inner CMS taking place sequentially during and following the Nevadan event. Emplacement of the outer CMS, and possibly the White Mountain inner CMS subunit, involved significant tectonic erosion as evidenced by the rootless aspect of upper plate plutons. Emplacement of the Dry Lake inner CMS subunit probably occurred some 10-20 Myr later. The absence of Josephine ophiolite and its Galice Formation cover from the inner CMS points to removal of these lithologies during underthrusting.

The far inboard position of these assemblages requires shallow-angle thrust emplacement, which we attribute to shallow-angle subduction. We further argue that the spatial restriction of the Nevadan event to the KMP plus northern Sierra Nevada, including deformation of the Josephine ophiolite but not the Coast Range ophiolite, is related to a relatively narrow (a few 100 km) corridor of shallow-angle subduction. The shallow-angle subduction must have been periodic to allow for sequential underplating of the outer CMS and both subunits of the inner CMS. In particular, the >10 Myr gap separating underplating of the White Mountain and Dry Lake subunits of the inner CMS, during which regional magmatism re-ignited before shutting down permanently when the Dry Lake subunit was emplaced, requires a phase of steeper subduction separating more shallowly-dipping intervals. The tectonic scenario in which episodic shallow-angle subduction took place is unclear, though may have been related to collision of separate thickened tracts of oceanic lithosphere ("tectonic switching" of Collins, 2002), buckling of the downgoing slab along mantle density interfaces (e.g., Schellart and Strak, 2021), or perhaps a combination of the two.

Shallow-angle emplacement of the CMS had profound effects on the KMP and adjacent geologic provinces in Late Jurassic and Early Cretaceous time. First, arc productivity waned during emplacement of the outer CMS and the White Mountain inner CMS subunit before shutting off entirely with the arrival of the Dry Lake subunit. Immediately following emplacement of the Dry Lake subunit, the entire KMP separated from the Sierran arc and was translated ~200 km to the west into the forearc. Westward displacement of the KMP coincided with regional cooling, low-angle normal faulting, and increasing sedimentation in the Great Valley forearc basin. We attribute these profound changes to rollback of the downgoing slab to a steeper trajectory, reducing interplate coupling and facilitating trenchward displacement of the entire KMP.

The parallels between Late Jurassic to Early Cretaceous tectonism recorded by the KMP and Late Cretaceous-early Cenozoic events of southern California are striking. In each location, the upper plate domain transitions from a phase of stable arc magmatism; yielding to diminishing magmatism, upper-mid crustal shortening, and basal crustal tectonic erosion plus underplating; and culminating with extensional collapse. These relations are inferred, in each location, to have resulted from a transition from relatively steeply-dipping to shallow-angle subduction and returning to a steeper dip. For the case of the KMP, at least three such tectonic switching events are inferred. Recognition of similar sequences of events in the geologic record may aid in the identification of additional ancient examples of shallow-angle subduction damage zones and improve our understanding of how modern "snapshots" of shallow-angle subduction zones may evolve.

7. ACKNOWLEDGEMENTS

This paper is dedicated to the memory of J. Saleeby (1948-2023) and J. D. Yule (1961-2022), to whom we are grateful for sharing their deep knowledge of Klamath geology. They are greatly missed. This effort benefitted from field and lab assistance by J. Anderson, A. Bleeker, R. Ceesay, J. Coons, R. DiCarlo, N. Sponseller, and K. Taylor; discussions with C. Barnes, W. Behr, T. Dumitru, W.G. Ernst, K. Gates, B. Hacker, G. Harper, M. Helper, C. Jacobson, J. MacDonald, K. Surpless, and C. Tewksbury-Christle. The manuscript was greatly improved through thoughtful reviews by A. Yoshinobu and K. Surpless. This work was supported by NSF grant EAR-1846811 (to Chapman). The Siskiyou Field Institute is thanked for providing a base of operations for fieldwork.

References Cited

Alberts, D., Gehrels, G.E., and Nelson, J., 2021, U-Pb and Hf analyses of detrital zircons from Paleozoic and Cretaceous Strata on Vancouver Island, British Columbia: Constraints on the Paleozoic tectonic evolution of southern Wrangellia: Lithosphere, https://doi.org/10.2113/2021/7866944.

Allen, C.M., and Barnes, C.G., 2006, Ages and some cryptic sources of Meso- zoic plutonic rocks in the Klamath Mountains, California and Oregon, *in* Snoke, A.W., and Barnes, C.G., eds., Geological Studies in the Klam- ath Mountains Province, California and Oregon: A Volume in Honor of William P. Irwin: Geological Society of America Special Paper 410, p. 223–245, https://doi.org/10.1130/2006.2410(11).

Arndt, N.T., 2013. The formation and evolution of the continental crust. Geochemical Perspectives, 2(3): 405-405.

Barnes, C.G., and Barnes, M.A., 2020, The western Hayfork terrane: Remnants of the Middle Jurassic arc in the Klamath Mountain province, California and Oregon: Geosphere, v. 16, no. 4, p. 1058–1081, https://doi.org/ 10.1130/GES02229.1.

Barnes, C.G., Petersen, S.W., Kistler, R.W., Prestvik, T., and Sundvoll, B., 1992, Tectonic implications of isotopic variation among Jurassic and Early Cretaceous plutons, Klamath Mountains: Geological Society of America Bulletin, v. 104, p. 117–126, https://doi.org/10.1130/0016-7606 (1992)104<0117:TIOIVA>2.3.CO;2.

Barnes, C.G., Petersen, S.W., Kistler, R.W., Murray, R., and Kays, M.A., 1996, Source and tectonic implications of tonalite-trondhjemite magmatism in the Klamath Mountains: Contributions to Mineralogy and Petrology, v. 123, p. 40–60, https://doi.org/10.1007/s004100050142.

Barnes, C.G., Mars, E.V., Swapp, S., and Frost, C.D., 2006, Petrology and geochemistry of the Middle Jurassic Ironside Mountain batholith: Evolution of potassic magmas in a primitive arc setting, in Snoke, A.W., and Barnes, C.G., eds., Geological Studies in the Klamath Mountains Prov- ince, California and Oregon: A Volume in Honor of William P. Irwin:

Geological Society of America Special Paper 410, p. 199–221, https://doi.org/10.1130/2006.2410(10).

Barrow, W.M., and Metcalf, R.V., 2006, A reevaluation of the paleotectonic significance of the Paleozoic Central Metamorphic terrane, eastern Klamath Mountains, California: New constraints from trace element geochemistry and 40Ar/39Ar thermochronology, *in* Snoke, A.W., and Barnes, C.G., eds., Geological Studies in the Klamath Mountains Province, California and Oregon: A Volume in Honor of William P. Irwin: Geological Society of America Special Paper 410, p. 393–410, https://doi .org/10.1130/2006.2410(19).

Barrows, A.G., 1969, Geology of the Hamburg-McGuffy Creek area Siskiyou County, California, and petrology of the Tom Martin ultramafic complex [Ph.D. thesis]: Los Angeles, University of California, 301 p.

Batt, G.E., Harper, G.D., Heizler, M., and Roden-Tice, M., 2010a, Creta- ceous sedimentary blanketing and tectonic rejuvenation in the western Klamath Mountains: Insights from thermochronology: Central Euro- pean Journal of Geosciences, v. 2, p. 138–151, https://doi.org/10.2478/ v10085-009-0041-4.

Batt, G.E., Casman, S.M., Garver, J., and Bigelow, J.J., 2010b, Thermotectonic evidence for the consequences of two-stage extension on the Trinity detachment surface, Eastern Klamath Mountains: American Journal of Science, v. 310, p. 261–281, https://doi.org/10.2475/04.2010.02.

Berge, P. A., Stauber, D. A. (1987) Seismic refraction study of upper crustal structure in the Lassen Peak Area, northern California. *Journal of Geophysical Research: Solid Earth*, 92. 10571-10579 doi:10.1029/jb092ib10p10571

Berkland, J.O., Raymond, L.A., Kramer, J.C., Moores, E.M., and O'Day, M., 1972, What is Franciscan?: AAPG Bulletin, v. 56, p. 2295a–2302, https:// doi.org/10.1306/819A421A-16C5-11D7-8645000102C1865D.

Bird, P., 1979. Continental delamination and the Colorado Plateau. J. Geophys. Res., 84: 7561-7571.

Black L, Kamo SL, Allen CM, Davis DW, Aleinikoff JN, et al. 2004. Improved 206Pb/238U microprobe geochronology by the monitoring of a trace-element-related matrix effect; SHRIMP, ID-TIMS, ELA-ICP-MS and oxygen isotope documentation for a series of zircon standards. Chem. Geol. 205:115–40

Blakey, R.C., and Ranney, W.D., 2018, Ancient Landscapes of Western North America: Cham, Switzerland, Springer, 228 p., https://doi.org/ 10.1007/978-3-319-59636-5.

Brown, E.H., and Blake, M.C., Jr., 1987, Correlation of early Cretaceous blue- schists in Washington, Oregon and northern California: Tectonics, v. 6, no. 6, p. 795–806, https://doi.org/10.1029/TC006i006p00795.

Brun, J. P., and C. Faccenna (2008), Exhumation of high-pressure rocks driven by slab rollback, *Earth planet. Sci. Lett.*, **272**, 1–7, doi:10.1016/j.epsl.2008.02.038.

Burchfiel, B.C., Cowan, D.S., and Davis, G.A., 1992, Tectonic overview of the Cordilleran orogen in the western United States, *in* Burchfiel, B.C., Lipman, P.W., and Zoback, M.L., eds., The Cordilleran Orogen: Conter- minous U.S.: Boulder, Colorado, Geological Society of America, Geol- ogy of North America, v. G3, p. 407–414, https://doi.org/10.1130/DNAG-GNA-G3.407.

Burton, W.C., 1982, Geology of the Scott Bar Mountains, northern California [M.S. thesis]: Eugene, University of Oregon, 120 p.

Cashman, S.M., and Elder, D.R., 2002, Post-Nevadan detachment faulting in the Klamath Mountains, California: Geological Society of America Bulletin, v. 114, p. 1520–1534, https://doi.org/10.1130/0016-7606(2002)114 <1520:PNDFIT>2.0.CO;2.

Chapman, A.D., 2017, The Pelona–Orocopia–Rand and related schists of southern California: A review of the best-known archive of shallow subduction on the planet: International Geology Review, v. 59, no. 5–6, p. 664–701, https://doi.org/10.1080/00206814.2016.1230836.

Chapman, J.B., Shields, J.E., Ducea, M.N., Paterson, S.R., Attia, S., and Ardill, K.E., 2021a, The causes of continental arc flare ups and drivers of episodic magmatic activity in Cordilleran orogenic systems: Lithos, v. 398–399, 106307, https://doi.org/10.1016/j.lithos.2021.106307.

Chapman, A.D., Yule, J.D., LaMaskin, T., Schwartz, W., 2021b, Middle Jurassic to Early Cretaceous tectonic evolution of the western Klamath Mountains and outboard Franciscan assemblages, northern California-southern Oregon: Geological Society of America Books.

Chen, J.H., and Moore, J.G., 1982, Uranium-lead isotopic ages from the Sierra Nevada batholith, California: Journal of Geophysical Research, v. 87, p. 4761–4784, https://doi.org/10.1029/JB087iB06p04761.

Coint, N., Barnes, C.G., Yoshinobu, A.S., Chamberlain, K.R., and Barnes, M.A., 2013, Batch-wise assembly and zoning of a tilted calc-alkaline batholith: Field relations, timing, and compositional variation: Geosphere, v. 9, p. 1729–1746, https://doi.org/10.1130/GES00930.1.

Clift, P., and P. Vannucchi, 2004, Controls on tectonic accretion versus erosion in subduction zones: Impli- cations for the origin and recycling of the continental crust, Rev. Geophys., 42, RG2001, doi:10.1029/ 2003RG000127.

Cloos, M., and R. L. Shreve, 1988, Subduction-channel model of prism accretion, melange formation, sediment subduction, and subduction erosion at convergent plate margins, 1, Background and description, Pure Appl. Geophys., 128, 455– 500.

Coleman, R.G., Manning, C.E., Mortimer, N., Donato, M.M., and Hill, L.B., 1988, Tectonic and regional metamorphic framework of the Klamath Mountains and adjacent Coast Ranges, California and Oregon, *in* Ernst, W.G., ed., Metamorphism and Crustal Evolution of the Western United States—Rubey Volume VII: Englewood Cliffs, New Jersey, Prentice Hall, p. 1059–1097.

Collins, W.J., 2002, Hot orogens, tectonic switching, and creation of continental crust. Geology, 30, 535–538.

Coney, P. J., and Reynolds, S. J., 1977, Cordilleran Benioff zones: Nature, v. 270, p. 403-405.

Constenius, K. N., R. A. Johnson, W. R. Dickinson, and T. A. Williams, 2000, Tectonic evolution of the Jurassic-Cretaceous Great Valley forearc, California: Implications for the Franciscan thrust-wedge hypothesis, Geol. Soc. Am. Bull., 112, 1703–1723, doi:10.1130/0016-7606(2000)112<1703: TEOTJC>2.0.CO;2.

Coutts, D.S., Matthews, W.A., Hubbard, S.M., 2019, Assessment of widely used methods to derive depositional ages from detrital zircon populations. Geosci. Front., 10 (4) (2019), pp. 1421-1435.

Darby, B.J., Wyld, S.J., and Gehrels, G.E., 2000, Provenance and paleogeogra- phy of the Black Rock terrane, northwestern Nevada, *in* Soreghan, M.J., and Gehrels, G.E., eds., Paleozoic and Triassic Paleogeography and Tec- tonics of Western Nevada and Northern California:

Geological Society of America Special Paper 347, p. 77–88, https://doi.org/10.1130/0-8137 -2347-7.77.

Davies JH, Stevenson DJ. 1992. Physical model of source region of subduction zone volcanics. J. Geophys. Res. 97:2037-70.

Davis, G.A., 1968, Westward thrust faulting in the south-central Klamath Moun- tains, California: Geological Society of America Bulletin, v. 79, p. 911–934, https://doi.org/10.1130/0016-7606(1968)79[911:WTFITS]2.0.CO;2.

DeCapitani, C.., Brown, T.H., 1987, The computation of chemical equilibria in complex systems containing non-ideal solutions, Geochim. Cosmochim. Acta 51 (1987) 2639 – 2652.

DeGraaff-Surpless K, Graham SA, Wooden JL, McWilliams MO, 2002, Detrital zircon provenance analysis of the Great Valley Group, California: Evolution of an arc-forearc system. Geol Soc Am Bull 114:1564-1580.

Dewey, J.F., 1981. Episodicity, sequence and style at convergent plate boundaries. The Continental Crust and Its Mineral Deposits. Special Paper, vol. 20. Geological Association of Canada, pp. 553–572.

Dickinson, W.R., and Gehrels, G.E., 2003, U-Pb ages of detrital zircons from Permian and Jurassic eolian sandstones of the Colorado Plateau, USA: Paleogeographic implications: Sedimentary Geology, v. 163, p. 29–66, https://doi.org/10.1016/S0037-0738(03)00158-1.

Dickinson, W.R., and Gehrels, G.E., 2008, U-Pb ages of detrital zircons in Jurassic eolian and associated sandstones of the Colorado Plateau: Evi- dence for transcontinental dispersal and intraregional recycling of sedi- ment: Geological Society of America Bulletin, v. 121, p. 408–433, https:// doi.org/10.1130/B26406.1.

Dickinson, W.R., and Gehrels, G.E., 2009, Use of U-Pb ages of detrital zircons to infer maximum depositional ages of strata: A test against a Colorado Plateau Mesozoic database: Earth and Planetary Science Letters, v. 288, p. 115–125, https://doi.org/10.1016/j.epsl.2009.09.013.

Dickinson, W.R., 2000, Geodynamic interpretation of Paleozoic tectonic trends oriented oblique to the Mesozoic Klamath-Sierran continental margin in California, *in* Soreghan, M.J., and Gehrels, G.E., eds., Paleozoic and Triassic Paleogeography and Tectonics of Western Nevada and Northern California: Geological Society of America Special Paper 347, p. 209–245, https://doi.org/10.1130/0-8137-2347-7.209.

Dickinson, W.R., 2004, Evolution of the North American Cordillera: Annual Review of Earth and Planetary Sciences, v. 32, p. 13–45, https://doi.org/ 10.1146/annurev.earth.32.101802.120257.

Donato, M.M., Barnes, C.G., and Tomlinson, S.L., 1996, The enigmatic Apple- gate Group of southwestern Oregon: Age, correlation, and tectonic affin- ity: Oregon Geology, v. 58, p. 79–91.

Donato, M.M., 1987, Evolution of an ophiolitic tectonic mélange, Marble Mountains, northern California Klamath Mountains: Geological Society of America Bulletin, v. 98, p. 448–464, doi: 10.1130/0016-7606(1987)98<448:EOAOTM>2.0.CO;2.

Ducea, M.N., Kidder, S., Chesley, J.T., and Saleeby, J., 2009, Tectonic underplating of trench sediments beneath magmatic arcs: The central California example: International Geology Review, v. 51, no. 1, p. 1–26. doi:10.1080/00206810802602767

Dumitru, T.A., Wright, J.E., Wakabayashi, J., and Wooden, J.L., 2010, Early Cretaceous transition from nonaccretionary behavior to strongly accre- tionary behavior within the

Franciscan subduction complex: Tectonics, v. 29, TC5001, https://doi.org/10.1029/2009TC002542.

Engebretson, D.C., Cox, A., and Thompson, G.A., 1984, Correlation of plate motions with continental tectonics: Laramide to Basin-Range: Tectonics, v. 3, no. 2, p. 115–119, https://doi.org/10.1029/TC003i002p00115.

Ernst, W.G., Wu, C., Lai, M., and Zhang, X., 2017, U-Pb ages and sedimentary provenance of detrital zircons from eastern Hayfork meta-argillites, Saw- yers Bar area, northwestern California: The Journal of Geology, v. 125, p. 33–44, https://doi.org/10.1086/689186.

Ernst, W.G., 1990, Accretionary terrane in the Sawyers Bar area of the Western Triassic and Paleozoic Belt, central Klamath Mountains, northern California, *in* Harwood, D. S., and Miller, M.M., eds., Paleozoic and Early Meso- zoic Paleogeographic Relations: Sierra Nevada, Klamath Mountains, and Related Terranes: Geological Society of America Special Paper 225, p. 297–306, https://doi.org/10.1130/SPE255-p297.

Ernst, W.G., 2013, Earliest Cretaceous Pacificward offset of the Klamath Mountains salient, NW California–SW Oregon: Lithosphere, v. 5, p. 151–159, https://doi.org/10.1130/L247.1.

Ernst, W.G., 2017, Geologic evolution of a Cretaceous tectonometamorphic unit in the Franciscan Complex, western California: International Geology Review, v. 59, no. 5–6, p. 563–576, https://doi.org/10.1080/ 00206814.2016.1201440.

Evarts, R.C., and Schiffman, P., 1983, Submarine hydrothermal metamorphism of the Del Puerto ophiolite, California: American Journal of Science, v. 283, p. 289–340. doi:10.2475/ajs.283.4.289

Ferrari L, Orozco-Esquivel T, Manea V, Manea M. 2012. The dynamic history of the Trans-Mexican Volcanic Belt and the Mexico subduction zone. Tectonophysics 522:122–49

Fuis, G.S., Zucca, J.J., Mooney, W.D., and Milkereit, B., 1987, A geologic interpretation of seismic-refraction results in northeastern California: Geological Society of America Bulletin, v. 98, p. 53–65, doi: 10.1130/0016-7606(1987)98<53:AGIOSR>2.0.CO;2.

Garlick, S.R., Medaris, L.G., Jr., Snoke, A.W., Schwartz, J.J., and Swapp, S.M., 2009, Granulite-to amphibolite-facies metamorphism and penetrative deformation in a disrupted ophiolite, Klamath Mountains, California: A deep view into the basement of an accreted oceanic arc, *in* Miller, R.B., and Snoke, A.W., eds., Crustal Cross Sections from the Western North American Cordillera and Elsewhere: Implications for Tectonic and Petrologic Processes: Geological Society of America Special Paper 456, p. 151–186, https://doi.org/10.1130/2009.2456(06).

Gates, K., Yoshinobu, A., Barnes, C.G., Dailey, S.R., and Leib, S., 2019, Inverted metamorphic gradients and cryptic contacts surrounding the enigmatic Condrey Mountain dome, Klamath Mountain province, CA and OR: Geological Society of America Abstracts with Programs, v. 51, no. 4, https://doi.org/10.1130/abs/2019CD-329660.

Gehrels, G.E., and Pecha, M., 2014, Detrital zircon U-Pb geochronology and Hf isotope geochemistry of Paleozoic and Triassic passive margin strata of western North America: Geosphere, v. 10, p. 49–65, https://doi .org/10.1130/GES00889.1.

Gehrels, G., Valencia, V., and Pullen, A., 2006, Detrital zircon geochronology by laser-ablation multicollector ICPMS at the Arizona Laserchron Center: The Paleontological Society Papers, v. 12, p. 67–76.

Gehrels, G., Valencia, V.A., and Ruiz, J., 2008, Enhanced precision, accuracy, efficiency, and spatial resolution of U-Pb ages by laser ablation–multicollector–inductively coupled plasma–

mass spectrometry: Geochemistry Geophysics Geosystems, v. 9, no. 3, doi:10.1029/2007GC001805.

Goodge, J.W., 1989, Polyphase metamorphic evolution of a Late Triassic subduction complex, Klamath Mountains, northern California: Ameri- can Journal of Science, v. 289, p. 874–943, https://doi.org/10.2475/ ajs.289.7.874.

Gradstein, F.M., Ogg, J.G., Schmitz, M.D., and Ogg, G.M., 2020, The Geologic Time Scale 2020: Amsterdam, Netherlands, Elsevier, 1357 p.

Grove, M., Jacobson, C.E., Barth, A.P., and Vucic, A., 2003, Temporal and spatial trends of Late Cretaceous–early Tertiary underplating of Pelona and related schist beneath southern California and southwestern Arizona, in Johnson, S.E., Patterson, S.R., Fletcher, J.M., Girty, G.H., Kimbrough, D.L., and Martin-Barajas, A., eds., Tectonic Evolution of Northwestern Mexico and the Southwestern USA: Boulder, Colorado, Geological Society of America Special Paper 374, p. 381–406.

Grove, M., Gehrels, G.E., Cotkin, S.J., Wright, J.E., and Zou, H., 2008, Non- Laurentian cratonal provenance of Late Ordovician eastern Klamath blue- schists and a link to the Alexander terrane, *in* Wright, J.E., and Shervais, J.W., eds., Ophiolites, Arcs, and Batholiths: A Tribute to Cliff Hopson: Geological Society of America Special Paper 438, p. 223–250, https://doi .org/10.1130/2008.2438(08).

Guffanti, M., Clynne, M.A., Muffler, L.J.P., 1996. Thermal and mass implications of magmatic evolution in the Lassen volcanic region, California, and minimum constraints on basalt influx to the lower crust. Journal of Geophysical Research 101, 3003–3013.

Gutscher, M.A., Spakman, W., Bijwaard, H., and Engdahl, E.R., 2000, Geodynamics of flat subduction: Seismicity and tomographic constraints from the Andean margin: Tectonics, v. 19, p. 814–833.

Hacker, B., and Ernst, W.G., 1993, Jurassic orogeny in the Klamath Mountains: A geochronological analysis, *in* Dunn, G., and McDougall, K., eds., Mesozoic Paleogeography of the Western United States–II: California, Society of Economic Paleontologists and Mineralogists, Pacific Section 71, p. 37–60.

Hacker, B.R., Donato, M.M., Barnes, C.G., McWilliams, M.O., and Ernst, W.G., 1995, Timescales of orogeny: Jurassic construction of the Klamath Moun- tains: Tectonics, v. 14, p. 677–703, https://doi.org/10.1029/94TC02454.

Hacker, B.R., Kelemen, P.B., and Behn, M.D., 2011, Differentiation of the continental crust by relamination: Earth and Planetary Science Letters, v. 307, p. 501–516.

Harper, G.D., and Wright, J.E., 1984, Middle to Late Jurassic tectonic evolution of the Klamath Mountains, California-Oregon: Tectonics, v. 3, p. 759– 772, https://doi.org/10.1029/TC003i007p00759.

Harper, G.D., Saleeby, J.B., and Heizler, M., 1994, Formation and emplacement of the Josephine ophiolite, and the age of the Nevadan orogeny in the Klamath Mountains, California-Oregon: U/Pb zircon and 40Ar/39Ar geochronology: Journal of Geophysical Research, v. 99, p. 4293–4321, https://doi.org/10.1029/93JB02061.

Harper, G.D., 1984, The Josephine ophiolite: Geological Society of America Bulletin, v. 95, p. 1009–1026, https://doi.org/10.1130/0016-7606 (1984)95<1009:TJONC>2.0.CO;2.

Harper, G.D., 2003, Fe-Ti basalts and propagating rift tectonics in the Josephine ophiolite: Geological Society of America Bulletin, v. 115, p. 771–787, https://doi.org/10.1130/0016-7606(2003)115<0771:FBAPTI>2.0.CO;2.

Helper, M., 1985, Structural, metamorphic and geochronologic constrains on the origin of the Condrey Mountain Schist, north central Klamath Mountains, northern California [Ph.D. dissertation]: University of Texas at Austin, 209 p.

Helper, M.A., 1986, Deformation and high P/T metamorphism in the central part of the Condrey Mountain window, north-central Klamath Mountains, California and Oregon, *in* Evans, B.W., and Brown, E.H., eds., Blueschists and Eclogites: Geological Society of America Memoir 164, p. 125–141, https://doi.org/10.1130/MEM164-p125.

Hill, L.B., 1984, A tectonic and metamorphic history of the north-central Klam- ath Mountains, California [Ph.D. thesis]: Stanford University, 248 p.

Hotz, P.E., 1979, Regional metamorphism in the Condrey Mountain quad- rangle, north-central Klamath Mountains, California: U.S. Geological Survey Professional Paper 1086, 25 p., https://doi.org/10.3133/pp1086.

Hotz, P.E., Lanphere, M.A., and Swanson, D.A., 1977, Triassic blueschist from northern California and north-central Oregon: Geology, v. 5, p. 659–663, doi: 10.1130/0091-7613(1977)5□659:TBFNCA□2.0.CO;2.

Irwin, W.P., 1960, Geologic reconnaissance of the northern Coast Ranges and Klamath Mountains, California, with a summary of the mineral resources: San Francisco, California Division of Mines Bulletin 179, 80 p.

Irwin, W.P., 1972, Terranes of the western Paleozoic and Triassic belt in the southern Klamath Mountains, California, *in* Geological Survey Research, 1972, Chapter C: U.S. Geological Survey Professional Paper 800-C, p. C103–C111, https://doi.org/10.3133/pp800C.

Irwin, W.P., 2003, Correlation of the Klamath Mountains and Sierra Nevada: U.S. Geological Survey Open-File Report 02-490, 2 map sheets, https:// pubs.usgs.gov/of/2002/0490/.

Irwin, W.P., and Wooden, J.L., 1999, Plutons and accretionary episodes of the Klamath Mountains, California and Oregon: Reston, Virginia, U.S. Geological Survey Open-File Report 99–0374, 1 sheet.

Jacobson, C.E., Grove, M., Vucic, A., Pedrick, J.N., and Ebert, K.A., 2007, Exhumation of the Orocopia Schist and associated rocks of southeastern California: Relative roles of erosion, synsubduction tectonic denudation, and middle Cenozoic extension: Geological Society of America Special Paper, v. 419, p. 1–37.

Jacobson, C.E., Grove, M., Pedrick, J.N., Barth, A.P., Marsaglia, K.M., Gehrels, G.E., and Nourse, J.A., 2011, Late Cretaceous-early Cenozoic tectonic evolution of the southern California margin inferred from provenance of trench and forearc sediments: Geological Society of America Bulletin, v. 123, no. 3–4, p. 485–506. doi:10.1130/B30238.1

Johnston, S.T., and Borel, G.D., 2007, The odyssey of the Cache Creek ter- rane, Canadian Cordillera: Implications for accretionary orogens, tectonic setting of Panthalassa, the Pacific superwell, and break-up of Pangea: Earth and Planetary Science Letters, v. 253, p. 415–428, https://doi.org/ 10.1016/j.epsl.2006.11.002.

Jones, D.L., and Irwin, W.P., 1971, Structural implications of an offset Early Cretaceous shoreline in northern California: Geological Society of America Bulletin, v. 82, p. 815–822, https://doi.org/10.1130/0016-7606(1971)82[815:SIOAOE]2.0.CO;2.

Kay, R.W. and Kay, S. Mahlburg, 1991. Creation and destruction of lower continental crust. Geol. Rundsch., 80(Z):259-278.

Klapper, M., and Chapman, A., 2017, Inverted metamorphism of the Condrey Mountain schist (northern California/southern Oregon): A ~30 myr record of subduction initiation and maturation beneath a cooling upper plate: Geological Society of America Abstracts with Programs, v. 49, no. 4, https://doi.org/10.1130/abs/2017CD-292952.

Klein, C.W., 1977, Thrust plates of the north-central Klamath Mountains near Happy Camp, California: California Division of Mines and Geology, Spe- cial Publication, v. 28, p. 23–26.

Lallemand, S., Peyret, M., van Rijsingen, E., Arcay, D., & Heuret, A. (2018). Roughness characteristics of oceanic seafloor prior to subduction in relation to the seismogenic potential of subduction zones. Geochemistry, Geophysics, Geosystems, 19(7), 2121–2146. https://doi.org/10.1029/2018gc007434

LaMaskin, T.A., Rivas, J.A., Barbeau, D.L., Schwartz, J.J., Russell, J.A., and Chapman, A.D., 2021, A crucial geologic test of Late Jurassic exotic col- lision versus endemic re-accretion in the Klamath Mountains province, western United States, with implications for the assembly of western North America: Geological Society of America Bulletin, https://doi.org/ 10.1130/B35981.1.

Lanphere, M.A., Irwin, W.P., and Hotz, P.E., 1968, Isotopic age of the Nevadan orogeny and older plutonic and metamorphic events in the Klamath Mountains, California: Geological Society of America Bulletin, v. 79, p. 1027–1052, https://doi.org/10.1130/0016-7606(1968)79[1027:IAOTNO]2.0.CO;2.

Liu, L., Gurnis, M., Seton, M., Saleeby, J., Müller, R.D., and Jackson, J., 2010, The role of oceanic plateau subduction in the Laramide orogeny: Nature Geoscience, v. 3, p. 353–357. doi:10.1038/ngeo829

Ludwig, K.R., 2003, Mathematical-statistical treatment of data and errors for 230Th/U geochronology: Reviews in Mineralogy and Geochemistry, v. 52, p. 631–656, doi:10.2113/0520631.

Lund, K., and Snee, L.W., 1988, Metamorphism, structural development, and age of the continent-island arc juncture in west-central Idaho, *in* Ernst, W.G., ed., Metamorphism and Crustal Evolution of the Western United States—Rubey Volume III: Englewood Cliffs, New Jersey, Prentice Hall, p. 297–331.

MacDonald, J.H., Jr., Harper, G.D., and Zhu, B., 2006, Petrology, geochemistry, and provenance of the Galice Formation, Klamath Mountains, Oregon and California, *in* Snoke, A.W., and Barnes, C.G., eds., Geological Stud- ies in the Klamath Mountains Province, California and Oregon: A Volume in Honor of William P. Irwin: Geological Society of America Special Paper 410, p. 77–101, https://doi.org/10.1130/2006.2410(04).

Manuszak, J.D., Satterfield, J.I., and Gehrels, G.E., 2000, Detrital-zircon geochronology of Upper Triassic strata in western Nevada, *in* Soreghan, M.J., and Gehrels, G.E., eds., Paleozoic and Triassic Paleogeography and Tec- tonics of Western Nevada and Northern California: Geological Society of America Special Paper 347, p. 109–118, https://doi.org/10.1130/0-8137 -2347-7.109.

Mauel, D.J., Lawton, T.F., González-León, C., Iriondo, A., and Amato, J.M., 2011, Stratigraphy and age of Upper Jurassic strata in north-central Sonora, Mexico: Southwestern Laurentian record of crustal extension and tectonic transition: Geosphere, v. 7, p. 390–414, https://doi.org/10.1130/ GES00600.1.

May, S.R., and Butler, R.F., 1986, North American Jurassic apparent polar wonder: Implications for plate motion, paleogeography and Cordilleran tectonics: Journal of Geophysical Research, v. 91, no b11, p. 11519-11544, https://doi.org/10.1029/JB091iB11p11519.

May, S.R., Beck, M.E., Jr., and Butler, R.F., 1989, North American apparent polar wander, plate motion, and left-oblique convergence:Late Jurassic-Early Cretaceous orogenic consequences: Tectonics, v. 8, p. 443-451.

McClelland, W.C., Gehrels, G.E., and Saleeby, J.B., 1992, Upper Jurassic– lower Cretaceous basinal strata along the Cordilleran margin: Implications for the accretionary history of the Alexander-Wrangellia-Peninsular terrane: Tectonics, v. 11, p. 823–835, https://doi.org/10.1029/92TC00241.

Medaris, L.G., Jr., 1966, Geology of the Seiad Valley area, Siskiyou County, California, and petrology of the Seiad ultramafic complex [Ph.D. thesis]: University of California, Los Angeles, 333 p.

Miller, M.M., and Saleeby, J.B., 1995, U-Pb geochronology of detrital zir- con from Upper Jurassic synorogenic turbidites, Galice Formation, and related rocks, western Klamath Mountains: Correlation and Klamath Mountains provenance: Journal of Geophysical Research, v. 100, B9, p. 18,045–18,058, https://doi.org/10.1029/95JB00761.

Miller MM. 1987. Dispersed remnants of a northeast Pacific fringing arc: Upper Paleozoic terranes of Permian McCloud faunal affinity, western U.S. Tectonics 6:807–30.

Moores, E.M., 1970, Ultramafics and orogeny, with models of the US Cor- dillera and the Tethys: Nature, v. 228, p. 837–842, https://doi.org/ 10.1038/228837a0.

Mortimer, N., and Coleman, R.G., 1985, A Neogene structural dome in the Klamath Mountains, California: Geology, v. 13, p. 253–256, https://doi .org/10.1130/0091-7613(1985)13<253:ANSDIT>2.0.CO;2.

Orme, D. A., & Surpless, K. D. (2019). The birth of a forearc: The basal Great Valley Group, California, USA. Geology, 47(8), 757–761.https://doi.org/10.1130/G46283.1

Paces, J.B. and Miller, J.D., 1993. Precise UPb ages of Duluth Complex and related mafic intrusions, northeastern Minnesota: Geochronological insights to physical, petrogenic, paleomagnetic, and tectonomagmatic processes associated with the 1.1 Ga Midcontinent Rift System. Journal of Geophysical Research, 98, no. B8, p. 13997-14013.

Pérez-Campos, X., Kim, Y., Husker, A., Davis, P.M., Clayton, R.W., Iglesias, A., Pacheco, J.F., Singh, S.K., Manea, V.C., Gurnis, M., 2008. Horizontal subduction and truncation of the Cocos Plate beneath central Mexico. Geophysical Research Letters 35, L18303. doi:10.1029/2008GL035127

Saleeby, J.B., and Harper, G.D., 1993, Tectonic relations between the Galice Formation and the schists of Condrey Mountain, Klamath Mountains, northern California, in Dunne, G., and McDougall, K., eds., Mesozoic Paleography of the Western United States–II: Los Angeles, California, Pacific Section, Society of Economic Paleontologists and Mineralogists, p. 61–80.

Saleeby, J.B., Harper, G.D., Snoke, A.W., and Sharp, W.D., 1982, Time rela- tions and structural-stratigraphic patterns in ophiolite accretion, west central Klamath Mountains, California: Journal of Geophysical Research, v. 87, p. 3831–3848, https://doi.org/10.1029/JB087iB05p03831.Saleeby, 2003

Saleeby, J., 2007, The western extent of the Sierra Nevada batholith in the Great Valley basement and its significance in underlying mantle dynamics: Eos (Transactions, American Geophysical Union), v. 88, no. 52, abs. T31E-02.

Schellart, W.P., and Strak, V., 2021, Geodynamic models of short lived, long-lived and periodic flat slab subduction: Geophysical Journal International , v. 226, p. 1517–1541, https://doi.org/10.1093/gji/ggab126.

Scherer, H.H., and Ernst, W.G., 2008, North Fork terrane, Klamath Mountains, California: Geologic, geochemical, and geochronologic evidence for an early Mesozoic forearc, *in* Wright, J.E., and Shervais, J.W., eds., Ophiolites, Arcs, and Batholiths: Geological Society of America Special Paper 438, p. 289–309, https://doi.org/10.1130/2008.2438(10).

Scherer, H.H., Ernst, W.G., and Wooden, J.L., 2010, Regional detrital zircon provenance of exotic metasandstone blocks, Eastern Hayfork terrane, western Paleozoic and Triassic belt, Klamath Mountains, California: The Journal of Geology, v. 118, p. 641–653, https://doi.org/10.1086/656352.

Scholl, D. W., and R. von Huene (2007), Crustal recycling at modern subduction zones applied to the past: Issues of growth and preservation of continental basement crust, mantle geochemistry, and super- continent reconstruction, in 4-D Framework of Continental Crust, edited by R. D. Hatcher Jr. et al., Mem. Geol. Soc. Am., 200, 9–32, doi:10.1130/2007.1200(02).

Scholl, D.W., and von Huene, R., 2009, Implications of estimated magmatic additions and recycling losses at the subduction zones of accretionary (non-collisional) and collisional (suturing) oro- gens, in Cawood, P., and Kröner, A., eds., Accretionary orogens in space and time: Geological Society of London, Special Publication 318, p. 105–125.

Schweickert, R.A., and Cowan, D.S., 1975, Early Mesozoic tectonic evolution of the western Sierra Nevada, California: Geological Society of Amer- ica Bulletin, v. 86, p. 1329–1336, https://doi.org/10.1130/0016-7606 (1975)86<1329:EMTEOT>2.0.CO;2.

Schweickert, R.A., Bogen, N.L., Girty, G.H., Hanson, R.E., and Merguerian, C., 1984, Timing and structural expression of the Nevadan orogeny, Sierra Nevada, California: Geological Society of America Bulletin, v. 95, p. 967–979, doi: 10.1130/0016-7606(1984)95<967:TASEOT>2.0.CO;2.

Seton, M., Müller, R.D., Zahirovic, S., Gaina, C., Torsvik, T., Shephard, G., Talsma, A., Gurnis, M., Turner, M., and Chandler, M., 2012, Global continental and ocean basin reconstructions since 200 Ma: EarthScience Reviews, v. 113, p. 212–270. doi:10.1016/j.earscirev.2012.03.002

Sharman, G.R., Sharman, J.P., and Sylvester, Z., 2018, A Python-based toolset for visualizing and analyzing detrital geo-thermochronologic data: The Depositional Record, v. 4, p. 202–215, https://doi.org/10.1002/dep2.45.

Shervais, J.W., Kimbrough, D.L., Renne, P., Hanan, B.B., Murchey, B., Snow, C.A., Zoglman-Schuman, M.M., and Beaman, J., 2004, Multi-stage origin of the Coast Range ophiolite, California: Implications for the life cycle of supra-subduction zone ophiolites: International Geology Review, v. 46, p. 289–315.

Snoke, A.W., and Barnes, C.G., 2006, The development of tectonic concepts for the Klamath Mountains province, California and Oregon, *in* Snoke, A.W., and Barnes, C.G., eds., Geological Studies in the Klamath Mountains Province, California and Oregon: A Volume in Honor of William P. Irwin: Geological Society of America Special Paper 410, p. 1–29, https:// doi.org/10.1130/2006.2410(01).

Snoke, A.W., 1977, A thrust plate of ophiolitic rocks in the Preston Peak area, Klamath Mountains, California: Geological Society of America Bulletin, v. 88, p. 1641–1659, https://doi.org/10.1130/0016-7606 (1977)88<1641:ATPOOR>2.0.CO;2.

Snow, C. A., J. Wakabayashi, W. G. Ernst, and J. L. Wooden (2010), Detrital zircon evidence for progressive underthrusting in Franciscan metagraywackes, west-central California, Geol. Soc. Am. Bull., 122, 282–291, doi:10.1130/B26399.1.

Speed, R.C., 1977, Island-arc and other paleogeographic terranes of late Paleo- zoic age in the western Great Basin, *in* Stewart, J.H., Stevens, C.H., and Fritsche, A.E., eds., Paleozoic Paleogeography of the Western United States: Pacific Section, Society of Economic Paleontologists and Mineralogists, p. 349–362.

Speed, R.C., 1979, Collided Paleozoic microplate in the western U.S.: The Journal of Geology, v. 87, p. 279–292, https://doi.org/10.1086/628417.

Stern, R.J., Scholl, D.W., 2010. Yin and yang of continental crust creation and destruction by plate tectoic processes. International Geology Review 52: 1-31.

Suppe, J., and Armstrong, R.L., 1972, Potassium-argon dating of Franciscan metamorphic rocks: American Journal of Science, v. 272, no. 3, p. 217– 233, https://doi.org/10.2475/ajs.272.3.217.

Surpless, K.D., Graham, S.A., Covault, J.A., and Wooden, J.L., 2006, Does the Great Valley Group contain Jurassic strata? Reevaluation of the age and early evolution of a classic forearc basin: Geology , v. 34, p. 21–24, https://doi.org/10.1130/G21940.1.

Tewksbury-Christle, C. M., Behr, W. M., & Helper, M. A., 2021, Tracking deep sediment underplating in a fossil subduction margin: Implications for interface rheology and mass and volatile recycling. Geochemistry, Geophysics, Geosystems, 22(3), 1–23. https://doi.org/10.1029/2020gc009463

Tipper, H.W., 1984, The allochthonous Jurassic-Early Cretaceous terranes of the Canadian Cordillera and their relation to correlative strata of the North American craton, *in* Jurassic-

Cretaceous Biochronology and Paleogeography of North America: Geological Association of Canada Special Paper 27, p. 113–120.

Underwood, M., Bachman, S. B. and Schweller, W. J., 1980, Sedimentary processes and facies associations within trench and trench-slope settings, in Field, M. E. and others, eds., Quaternary depositional environments on the Pacific continental margin: Society of Economic Paleontologists and Mineralogists, Pacific Section, p. 211-229.

Vermeesch, P. (2012). On the visualisation of detrital age distributions. Chemical Geology, 312–313, 190–194. https://doi.org/10.1016/j.chemgeo.2012.04.021

Vermeesch, P. (2013). Multi-sample comparison of detrital age distributions. Chemical Geology, 341, 140–146.

Vermeesch, P. (2021). Maximum depositional age estimation revisited. Geoscience Frontiers, 12(2), 843–580. https://doi.org/10.1016/j.gsf.2020.08.008

von Huene, R., and Lallemand, S., 1990, Tectonic erosion along the Japan and Peru convergent margins: Geological Society of America Bulletin, v. 102, p. 704-720.

von Huene, R., and D. W. Scholl, 1991, Observations at convergent margins concerning sediment subduction, subduction erosion, and the growth of continental crust, Rev. Geophys., 29, 279–316, doi:10.1029/91RG00969.

Wakabayashi, J., 2015, Anatomy of a subduction complex: Architecture of the Franciscan Complex, California, at multiple length and time scales: Inter- national Geology Review, v. 57, no. 5–8, p. 669–746, https://doi.org/10 .1080/00206814.2014.998728.

Wallin, E.T., and Metcalf, R.V., 1998, Supra-subduction zone ophiolite formed in an extensional forearc: Trinity terrane, Klamath Mountains, California: The Journal of Geology, v. 106, p. 591–608, https://doi.org/ 10.1086/516044.

Wallin, E.T., Noto, R.C., and Gehrels, G.E., 2000, Provenance of the Ante- lope Mountain Quartzite, Yreka terrane, California: Evidence for large-scale late Paleozoic sinistral displacement along the North American Cordilleran margin and implications for the mid-Paleozoic fringing-arc model, in Soreghan, M.J., and Gehrels, G.E., eds., Paleozoic and Triassic Paleogeography and Tectonics of Western Nevada and Northern California: Geological Society of America Special Paper 347, p. 119–131, https://doi.org/10.1130/0-8137-2347-7.119.

Wernicke, B., and Klepacki, D.W., 1988, Escape hypothesis for the Stikine block: Geology, v. 16, p. 461–464, https://doi.org/10.1130/0091-7613 (1988)016<0461:EHFTSB>2.3.CO;2.

Wolf, M.B., and Saleeby, J.B., 1995, Late Jurassic dike swarms in the south- western Sierra Nevada Foothills terrane, California: Implications for the Nevadan orogeny and North American plate motion, *in* Miller, D.M., and Busby, C., eds., Jurassic Magmatism and Tectonics of the North American Cordillera: Geological Society of America Special Paper 299, p. 203–228, https://doi.org/10.1130/SPE299-p203.

Wright, J.E., and Fahan, M.R., 1988, An expanded view of Jurassic orogenesis in the western United States Cordillera: Middle Jurassic (pre-Nevadan) regional metamorphism and thrust faulting within an active arc environment, Klamath Mountains, California: Geological Society of America Bulletin, v. 100, p. 859–876, https://doi.org/10.1130/0016-7606 (1988)100<0859:AEVOJO>2.3.CO;2.

Wright, J.E., and Wyld, S.J., 1986, Significance of xenocrystic Precambrian zircon contained within the southern continuation of the Josephine ophiolite: Devils Elbow ophiolite remnant, Klamath Mountains, northern California: Geology, v. 14, p. 671–674, https://doi.org/10.1130/0091-7613 (1986)14<671:SOXPZC>2.0.CO;2.

Wright, J.E., and Wyld, S.J., 1994, The Rattlesnake Creek terrane, Klamath Mountains, California: An early Mesozoic volcanic arc and its basement of tectonically disrupted oceanic crust: Geological Society of America Bulletin, v. 106, p. 1033–1056, https://doi.org/10.1130/0016 -7606(1994)106<1033:TRCTKM>2.3.CO;2.

Wright, J.E., and Wyld, S.J., 2006, Gondwanan, Iapetan, Cordilleran interac- tions: A geodynamic model for the Paleozoic tectonic evolution of the North American Cordillera, *in* Haggart, J.W., Enkin, R.J., and Monger, J.W.H., eds., Paleogeography of the North American Cordillera: Evidence For and Against Large-Scale Displacements: Geological Association of Canada Special Paper 46, p. 377–408.

Wright, J.E., 1982, Permo-Triassic accretionary subduction complex, south-western Klamath Mountains, northern California: Journal of Geophysical Research, v. 87, p. 3805–3818, https://doi.org/10.1029/JB087iB05p03805.

Wyld, S.J., Rogers, J.W., and Copeland, P., 2003, Metamorphic evolution of the Luning-Fencemaker fold-thrust belt, Nevada: Illite crystallinity, metamorphic petrology, and 40Ar/39Ar geochronology: The Journal of Geology, v. 111, p. 17–38, https://doi.org/10.1086/344663.

Wyld, S.J., 1991, Permo-Triassic tectonism in volcanic arc sequences of the western U.S. Cordillera and implications for the Sonoman orogeny: Tectonics, v. 10, p. 1007–1017, https://doi.org/10.1029/91TC00863.

Wyld, S.J., 2002, Structural evolution of a Mesozoic back-arc fold-thrust belt in the U.S. Cordillera: New evidence from northern Nevada: Geological Society of America Bulletin, v. 114, p. 1452–1468, https://doi.org/ 10.1130/0016-7606(2002)114<1452:SEOAMB>2.0.CO;2.

Yule J.D., Saleeby, J.S., and Barnes, C.G., 2006, A rift-edge facies of the Late Jurassic Rogue–Chetco arc and Josephine ophiolite, Klamath Mountains, Oregon, *in* Snoke, A.W., and Barnes, C.G., eds., Geological Studies in the Klamath Mountains Province, California and Oregon: A Volume in Honor of William P. Irwin: Geological Society of America Special Paper 410, p. 53–76, https://doi.org/10.1130/2006.2410(03).

Figures

Figure 1. Simplified geologic and tectonic map of the Klamath Mountains province (KMP), modified after Blake et al. (1985) and Snoke and Barnes (2006), with sampled locations (white stars) overlain. Traces of cross-sections A–A′ and B–B′ (Fig. 2) overlain. Inset abbreviations: bm—Blue Mountains; ns—northern Sierra. Map abbreviations: C—China Peak complex; P—Preston Peak complex; IM— Ironside Mountain batholith; V— Vesa Bluffs pluton; .

Figure 2. (A) Simplified geologic map of the central Klamath Mountains Province, modified after Hotz (1969), Barrows (1969), Hill (1984), Burton (1982), Helper (1986), and Saleeby and Harper (1993). Note that many faults identified with thrust symbols have been variably reactivated in a normal sense. Amphibole 40Ar/39Ar ages from Saleeby and Harper (1993), Hacker and Ernst (1993), Hacker et al. (1995), and Donato et al. (1996). Zircon U-Pb ages from Snoke and Barnes (2006). See Figure 1 for map location. Sampled locations (white-filled circles) overlain; sample numbers correspond to those in Table 1. Abbreviations: CP—China Peak; DL—Dry Lake; TO—Trinity ophiolite; WM—White Mountain; CMsz—Condrey Mountain shear zone. (B) Cross-sections across the Condrey Mountain schist window (vertical = horizontal scale). Colors and symbols correspond to those used on Figure 2A. See Figure 1 for locations of section lines. Abbreviations: CIf—Condrey Internal fault; CMS—Condrey Mountain schist;

CRf—Coast Range fault; MSL—mean sea-level; Of—Orleans fault; SCf—Salt Creek fault; WPf—Wilson Point fault.

Figure 3. Simplified geologic map of the Scott River appendage, modified after Hotz (1979), Barrows (1969), Cornwall (1981), Burton (1982), Saleeby and Harper (1993). Map base: U.S. Geological Survey 30×60 min series (1:100,000 scale) maps of Yreka (1979) and Happy Camp (1983) quadrangles (The National Geologic Map Database: https://ngmdb.usgs.gov). Sampled localities overlain. See Figure 2A for map location.

Figure 4. Thin section photomicrographs of petrologic and structural features in the Condrey Mountain Schist and adjacent lithologies. (A) Transitional blueschist-greenschist facies metabasalt from the Dry Creek subunit. Plane-polarized light. (B) Disharmonic folds in Dry Lake metasedimentary rocks. Plane-polarized light. Circular “spotlight” inset shows cross-polarized light. (C) Intrafolial isoclinal folds in metasedimentary rocks from the White Mountain subunit. Plane-polarized light. (D) Highly cleaved (dark) and microlithon (light green) domains in semipelitic rocks of the outer Condrey Mountain Schist. Plane-polarized light. Spotlight shows cross-polarized light. (E) Garnet-bearing Gold Flat amphibolite. Plane-polarized light. Note tapered deformation twins in plagioclase plus amoeboid grain boundaries in undulose quartz (both shown in cross-polarized light spotlights), suggesting deformation at elevated shear stress and temperature. (F) Large garnet porphyroblast in Gold Flat amphibolite, (note garnet in this unit locally achieves diameters of ~1 cm). Plane-polarized light. (G) Leucogneiss of the outer Condrey Mountain Schist exposed north of Scott Bar showing plagioclase- and mica-dominated assemblage. Chlorite pseudomorph after pyrite at center. Plane-polarized light. (H) Metasedimentary assemblages of uncertain origin exposed along Klamath River assemblage. Note ruptured isoclinal fold adjacent to “cm” annotation. Plane-polarized light. Mineral abbreviations: Ab—albite; Act—actinolite; Bt—biotite; cm—carbonaceous material; Chl—chlorite; Ep—epidote; Gln—sodic amphibole (glaucophane/ crossite); Grt—garnet; Hbl—hornblende; Ilm—ilmenite; Pl—plagioclase; Py—pyrite; Qtz—quartz; wm—white (phengitic) mica.

Figure 5. Calculated P–T pseudosections for (a) inner and (b) outer CMS compositions. Dry Creek P-T estimate of Helper (1986) overlain in (a). Gold Flat P-T estimate of Klapper and Chapman (2017) overlain in (b). Modeled bulk compositions from Hotz (1979).

Figure 6. U-Pb zircon concordia plots (from laser ablation inductively coupled plasma mass spectrometry analysis) from (A) Gold Flat amphibolite melanosomes and (B) leucogneiss collected from ~0.4 miles north of Scott Bar (Fig. 3). Individual analyses shown as unfilled black ellipses; calculated concordia ages shown as white ellipses with black fill. MSWD—mean square of weighted deviates.

Figure 7. (A) Cumulative probability plot and (B) corresponding normalized kernel density estimates (KDE) with 10 Myr bandwidth comparing detrital zircon ages from samples collected from the Condrey Mountain schist. Note the split horizontal axis at 300 Ma and that spectra between 300 and 3000 Ma are vertically exaggerated by a factor of five. Pie diagram bin colors correspond to those beneath each KDE curve. Maximum depositional age ranges from Table 2. Uncertainties provided are 2σ. n—number of concordant analyzed grains.

Figure 8. (A) Cumulative probability plot (CPP) and (B) corresponding normalized kernel density estimates (KDE) with 10 Myr bandwidth comparing detrital zircon ages from samples collected from forearc, arc, and backarc domains of the Middle Jurassic–Early Cretaceous Klamath Mountains Province. Note the split horizontal axis at 300 Ma and that spectra between 300 and 3000 Ma are vertically exaggerated by a factor of five. Numbers in (A) correspond to those adjacent to curves in (B). Pie diagram bin colors correspond to those beneath each KDE curve. Abbreviations: N—number of analyzed samples; n—number of concordant analyzed grains. Data sources: 1) and 2) this study; 3) Dumitru et al. (2010); Schmidt and Chapman (in prep); 4a) Lamaskin et al. (2021); Surpless et al. (2023); 5) Gehrels and Miller (2000); Wallin et al. (2000); Grove et al. (2008), Scherer and Ernst (2008); Scherer et al. (2010); Ernst et al. (2017); 6) Orme and Surpless (2019); 7) Manuszak et al. (2000); Darby et al. (2000); Gehrels and Pecha (2014); 8) Dickinson and Gehrels (2009); 9) Alberts et al. (2021).

Figure 9. Multi-dimensional scaling (MDS) plot with samples plotted as pie diagrams. Pie diagram bin colors correspond to those beneath KDE curves in figs. 7 and 8. Axes are dimensionless D_{max} distances (Vermeesch, 2013). Data sources: samples 1-7 (Tables 1 and 2) – this study; CEk (Mesozoic and older rocks of the central and eastern Klamaths) - Gehrels and Miller (2000); Wallin et al. (2000); Grove et al. (2008), Scherer and Ernst (2008); Scherer et al. (2010); Ernst et al. (2017); Erg – Dickinson and Gehrels (2009); Galice (Galice Formation) – LaMaskin et al. (2021); Surpless et al. (2023); GVG (Great Valley Group) – Orme et al. (2019);

RCt (Rattlesnake Creek terrane cover) – LaMaskin et al. (2021); SFMS (South Fork Mountain schist) - Dumitru et al. (2010); Schmidt and Chapman (in prep); TrNV (Triassic backarc rocks) - ; Wrangellia - Alberts et al. (2021).

Figure 10. Summary of regional ages and events as well as maximum depositional ages from this study. Timing of KMP (Klamath Mountains Province) tectonic events compiled from sources given in the text. Maximum depositional ages (youngest single grain, YSG; youngest statistical population, YSP; and maximum likelihood algorithm, MLA) and associated uncertainties from Table 2. Igneous ages from U-Pb zircon analysis (Fig. 6). Jurassic and Cretaceous boundary ages from Gradstein et al. (2020). E—Early; M—Middle; L— Late; RCt—Rattlesnake Creek terrane. Barr.— Barremian, Haut. — Hauterivian, Val. — Valanginian, Berr.— Berriasian, Tith.—Tithonian, Kimm.—Kimmeridgian, Oxfor.—Oxfordian, Callov.—Callovian, Baj.—Bajocian, Bath.—Bathonian, Aal.— Aalenian, Toar.—Toarcian.

Figure 11. Model for Middle Jurassic to Early Cretaceous development of the KMP. At 180 Ma, Sawyers Bar terrane and outboard Rattlesnake Creek terrane dock with previously accreted Eastern Klamath, Central Metamorphic, and Fort Jones-Stuart Fork terranes. Slip along Siskiyou fault (Sf) occurs. At 175 Ma, trench retreats due to decreased upper-lower plate coupling. Onion Camp complex rifts from Rattlesnake Creek terrane, producing Preston Peak and China Peak mafic complexes. Western Hayfork arc initiates. At 170 Ma, trench advances and coupling drives Siskiyou orogeny and slip along the Wilson Point fault (WPf), invasion of Ironside batholith closely post-dates deformation. At 165 Ma trench retreats due to reduced coupling. Trench retreat initiates upper plate extension and formation of the Josephine ophiolite. Hemipelagic section of Galice formation, sourced primarily from the KMP, fills Josephine ophiolite-floored basin. At 160 Ma, extension and associated ophiolite formation and basin filling continue, upper plate magmatism flanks the east (Wooley Creek) and west (Rogue-Chetco) sides of the ophiolite-floored basin. At 155 Ma, rifting and arc magmatism each terminate as upper-lower plate coupling increases, driving the Nevadan event and thrusting along the Orleans fault (Of). KMP-derived and extraregional detritus fills the Josephine ophiolite-floored basin as the basin closes. At 150 Ma, Nevadan deformation culminates with thrusting along the Madstone Cabin fault (MCf). At 145 Ma, the predominantly mafic Western Klamath suite ignites as local and extraregional detritus continues to accumulate along the margin,

forming the proto-Franciscan/Inner CMS accretionary wedge. At 140 Ma, the trench continues to roll back and intermediate magmatism (TTG – tonalite-trondhjemite-granodiorite) occurs across the KMP. Franciscan/Inner CMS detritus continues to accumulate in the growing wedge. At 135 Ma, protoliths of the CMS begin underthrusting the KMP at low-angle, removing the lower crust via tectonic erosion. The driver of shallow-angle subduction is unknown. Thickened oceanic lithosphere is offered as a possibility. At 130 Ma, the trench rolls back, precipitating upper plate normal faulting along the Paskenta/Elder Creek/Cold Fork (PECCF) fault, possibly facilitated by removal of isostatically compensating lower crust in the 135 Ma panel, and relocating the KMP from the arc to the forearc. Basal Great Valley Group (GVG) detritus blanket the subdued Early Cretaceous topography of the KMP.

Figure 1

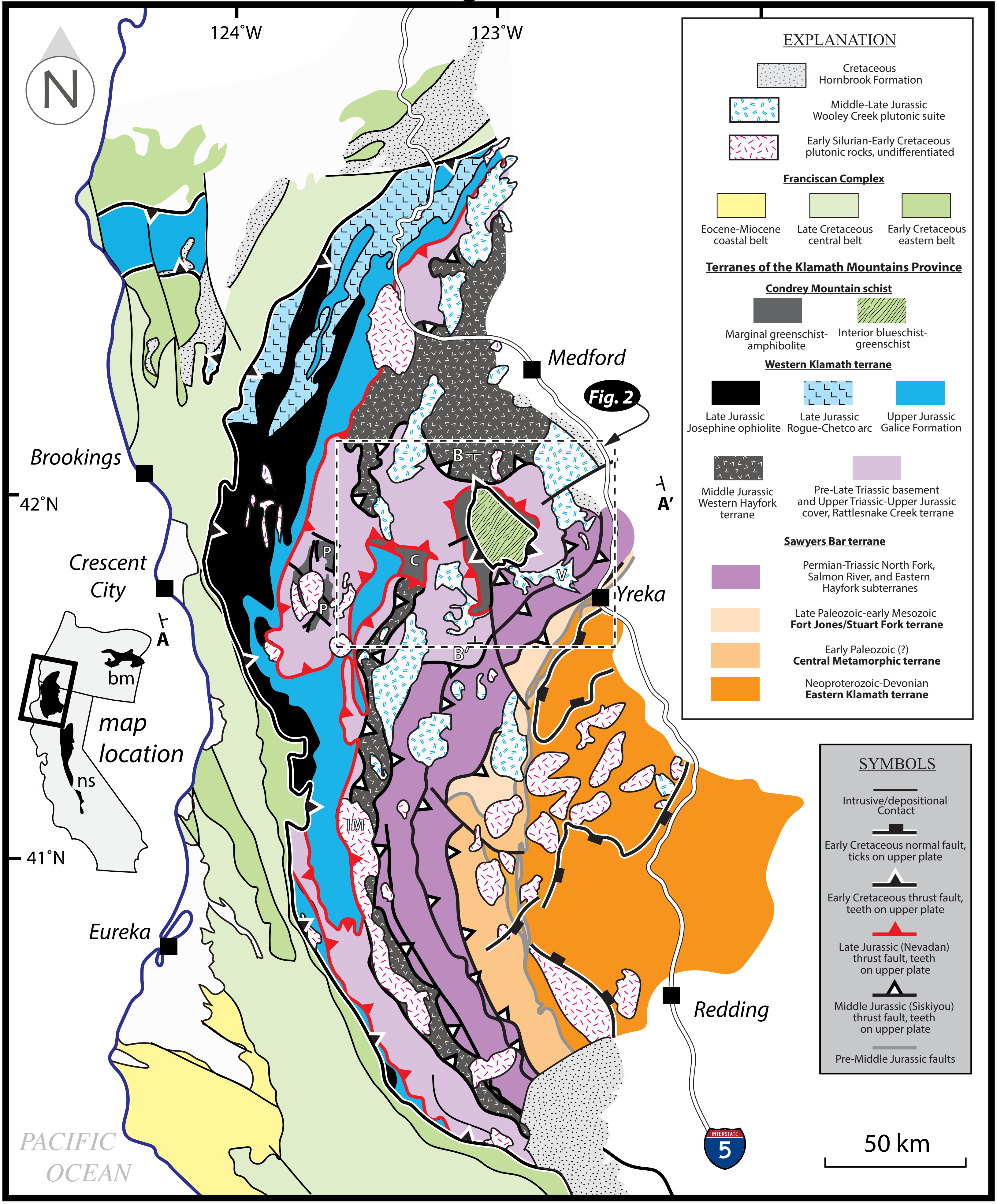

124˚W
123˚W
42˚N
41˚N
N
Medford
Fig. 2
Brookings
Crescent City
Yreka
Eureka
Redding
A
A'
B
B'
P
C
V
IM
bm
ns
map location
PACIFIC OCEAN
INTERSTATE 5
50 km
EXPLANATION
Cretaceous Hornbrook Formation
Middle-Late Jurassic Wooley Creek plutonic suite
Early Silurian-Early Cretaceous plutonic rocks, undifferentiated
Franciscan Complex
Eocene-Miocene coastal belt
Late Cretaceous central belt
Early Cretaceous eastern belt
Terranes of the Klamath Mountains Province
Condrey Mountain schist
Marginal greenschist-amphibolite
Interior blueschist-greenschist
Western Klamath terrane
Late Jurassic Josephine ophiolite
Late Jurassic Rogue-Chetco arc
Upper Jurassic Galice Formation
Middle Jurassic Western Hayfork terrane
Pre-Late Triassic basement and Upper Triassic-Upper Jurassic cover, Rattlesnake Creek terrane
Sawyers Bar terrane
Permian-Triassic North Fork, Salmon River, and Eastern Hayfork subterranes
Late Paleozoic-early Mesozoic Fort Jones/Stuart Fork terrane
Early Paleozoic (?) Central Metamorphic terrane
Neoproterozoic-Devonian Eastern Klamath terrane
SYMBOLS
Intrusive/depositional Contact
Early Cretaceous normal fault, ticks on upper plate
Early Cretaceous thrust fault, teeth on upper plate
Late Jurassic (Nevadan) thrust fault, teeth on upper plate
Middle Jurassic (Siskiyou) thrust fault, teeth on upper plate
Pre-Middle Jurassic faults

Figure 2a

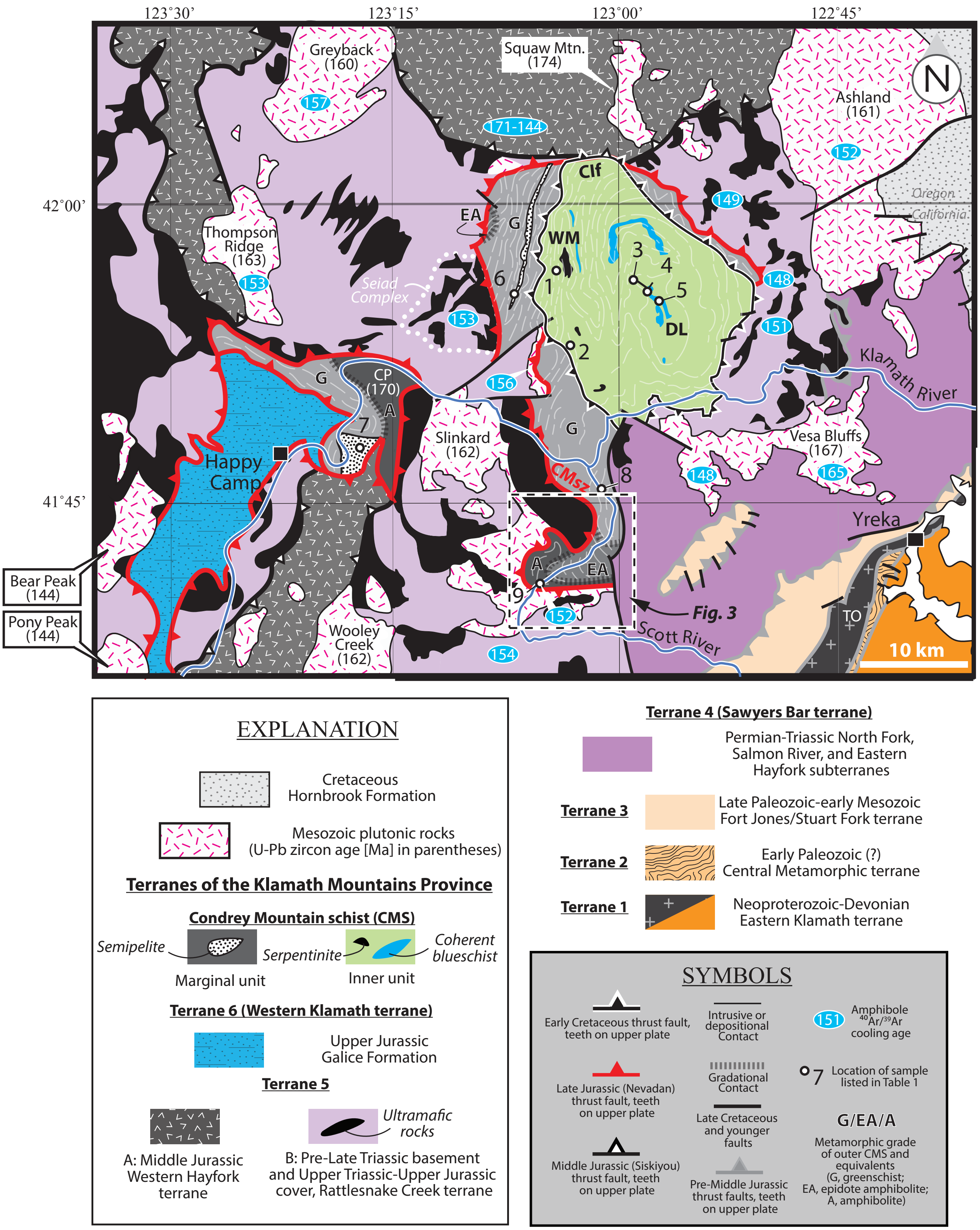

123°30'
123°15'
123°00'
122°45'
42°00'
41°45'
Greyback
(160)
Squaw Mtn.
(174)
Ashland
(161)
N
Oregon
California
Thompson
Ridge
(163)
Seiad
Complex
Clf
WM
DL
EA
G
CP
(170)
A
Happy
Camp
Slinkard
(162)
Vesa Bluffs
(167)
Klamath River
CMsz
Yreka
Fig. 3
Scott River
TO
10 km
Bear Peak
(144)
Pony Peak
(144)
Wooley
Creek
(162)
157
171-144
152
149
148
153
151
156
165
154
1
2
3
4
5
6
7
8
9
EXPLANATION
Cretaceous
Hornbrook Formation
Mesozoic plutonic rocks
(U-Pb zircon age [Ma] in parentheses)
Terranes of the Klamath Mountains Province
Condrey Mountain schist (CMS)
Semipelite
Serpentinite
Coherent
blueschist
Marginal unit
Inner unit
Terrane 6 (Western Klamath terrane)
Upper Jurassic
Galice Formation
Terrane 5
Ultramafic
rocks
A: Middle Jurassic
Western Hayfork
terrane
B: Pre-Late Triassic basement
and Upper Triassic-Upper Jurassic
cover, Rattlesnake Creek terrane
Terrane 4 (Sawyers Bar terrane)
Permian-Triassic North Fork,
Salmon River, and Eastern
Hayfork subterranes
Terrane 3
Late Paleozoic-early Mesozoic
Fort Jones/Stuart Fork terrane
Terrane 2
Early Paleozoic (?)
Central Metamorphic terrane
Terrane 1
Neoproterozoic-Devonian
Eastern Klamath terrane
SYMBOLS
Early Cretaceous thrust fault,
teeth on upper plate
Intrusive or
depositional
Contact
151
Amphibole
$^{40}Ar/^{39}Ar$
cooling age
Late Jurassic (Nevadan)
thrust fault, teeth
on upper plate
Gradational
Contact
7
Location of sample
listed in Table 1
Late Cretaceous
and younger
faults
G/EA/A
Metamorphic grade
of outer CMS and
equivalents
(G, greenschist;
EA, epidote amphibolite;
A, amphibolite)
Middle Jurassic (Siskiyou)
thrust fault, teeth
on upper plate
Pre-Middle Jurassic
thrust faults, teeth
on upper plate

Figure 2b

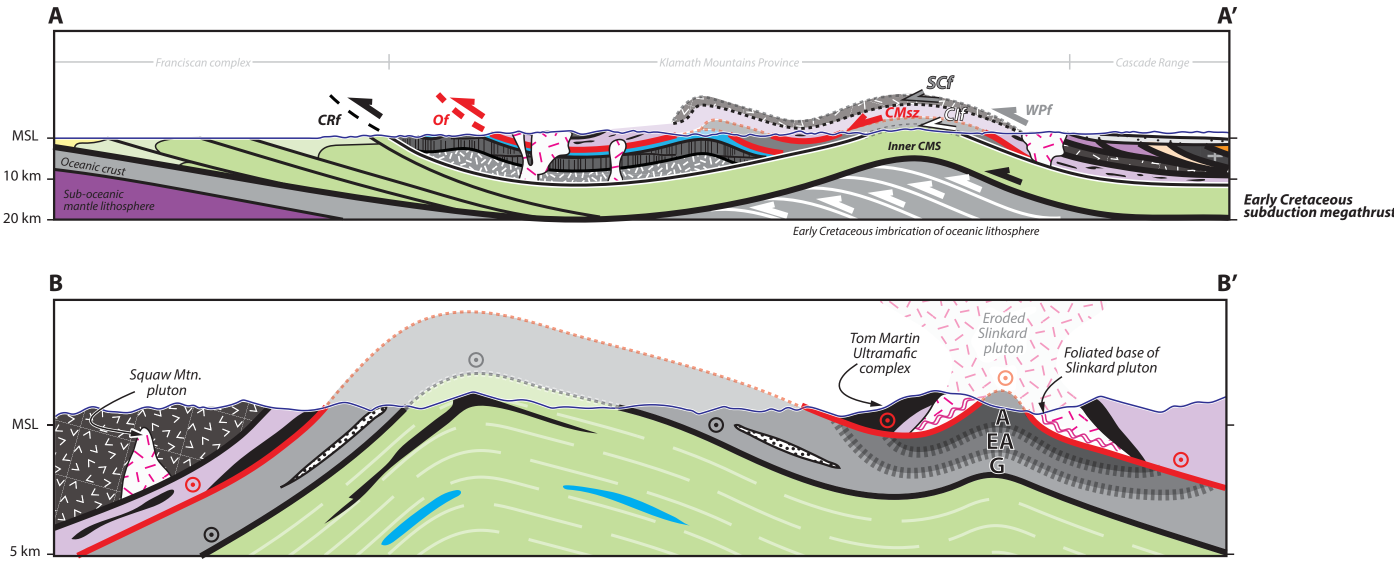
A
A'
Franciscan complex
Klamath Mountains Province
Cascade Range
SCf
CMsz
Clf
WPf
CRf
Of
MSL
10 km
20 km
Oceanic crust
Sub-oceanic mantle lithosphere
Inner CMS
Early Cretaceous subduction megathrust
Early Cretaceous imbrication of oceanic lithosphere
B
B'
Squaw Mtn. pluton
Tom Martin Ultramafic complex
Eroded Slinkard pluton
Foliated base of Slinkard pluton
A
EA
G
MSL
5 km

Figure 3

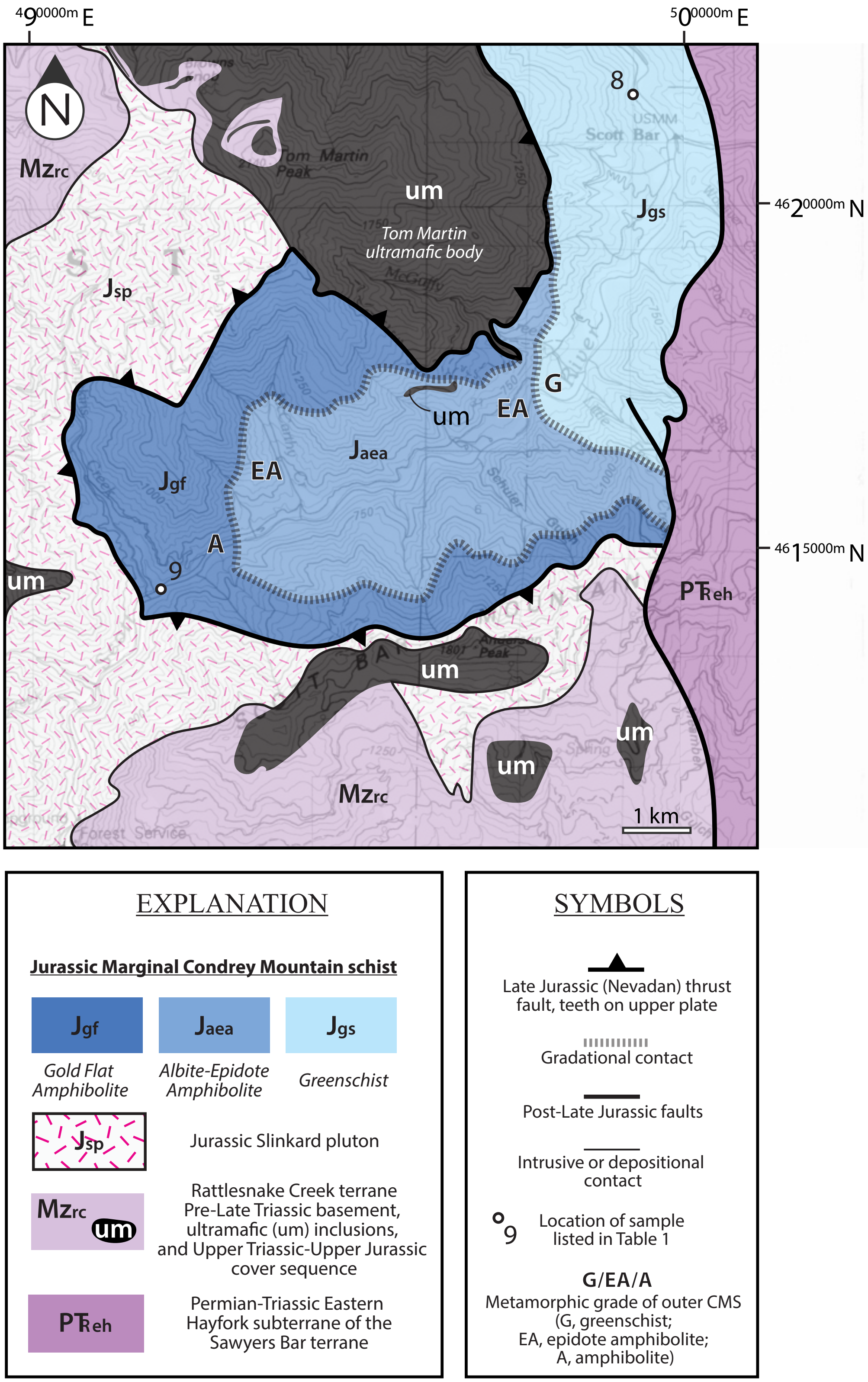

490000m E
500000m E
4620000m N
4615000m N
N
Mzrc
Jsp
um
Tom Martin ultramafic body
Tom Martin Peak
Scott Bar
8
Jgs
G
EA
Jaea
Jgf
A
9
PTReh
Anderson Peak
1 km
EXPLANATION
Jurassic Marginal Condrey Mountain schist
Jgf
Gold Flat Amphibolite
Jaea
Albite-Epidote Amphibolite
Jgs
Greenschist
Jsp
Jurassic Slinkard pluton
Mzrc
um
Rattlesnake Creek terrane Pre-Late Triassic basement, ultramafic (um) inclusions, and Upper Triassic-Upper Jurassic cover sequence
PTReh
Permian-Triassic Eastern Hayfork subterrane of the Sawyers Bar terrane
SYMBOLS
Late Jurassic (Nevadan) thrust fault, teeth on upper plate
Gradational contact
Post-Late Jurassic faults
Intrusive or depositional contact
9
Location of sample listed in Table 1
G/EA/A
Metamorphic grade of outer CMS (G, greenschist; EA, epidote amphibolite; A, amphibolite)

Figure 4

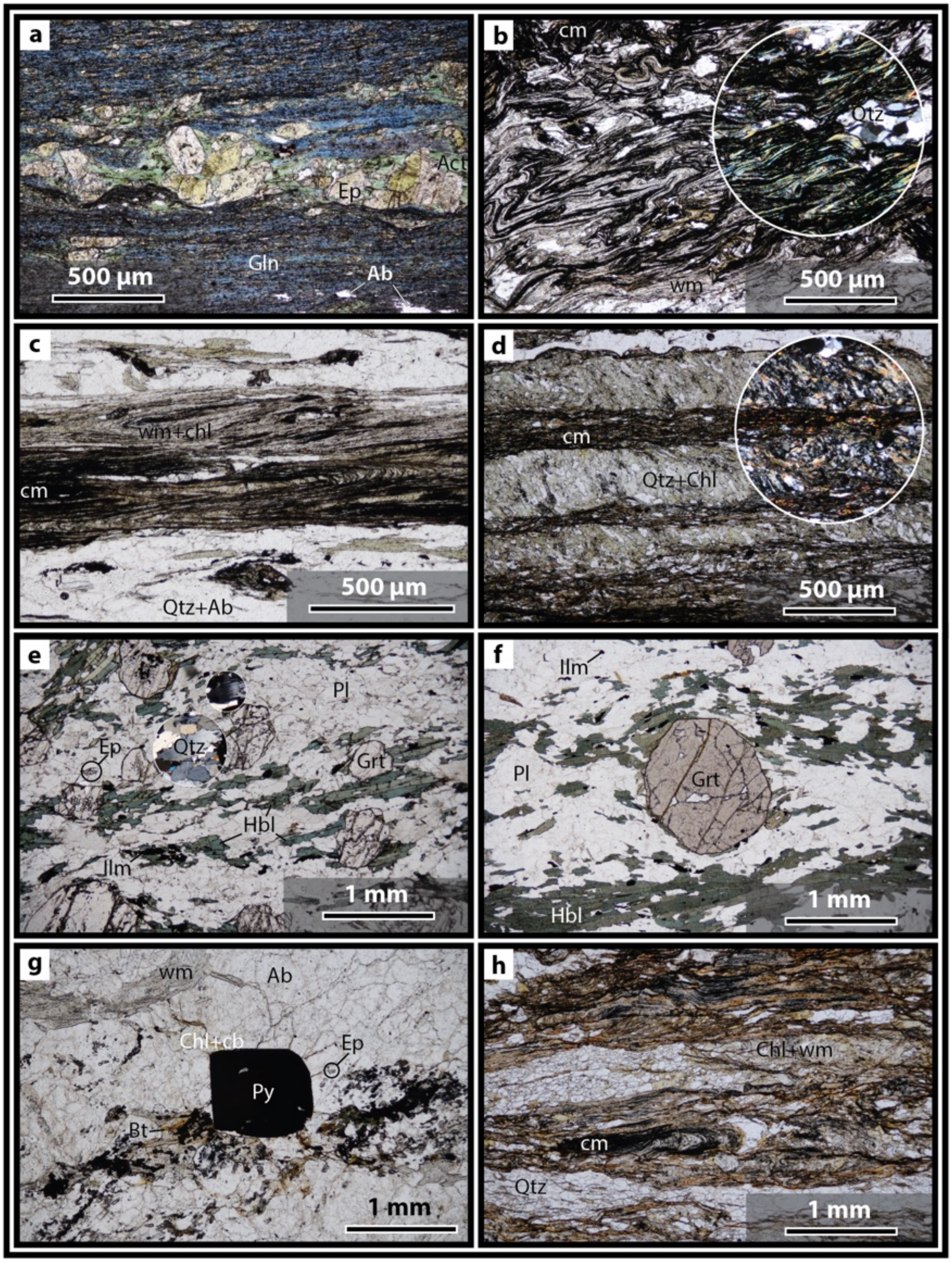

a
Act
Ep
Gln
Ab
500 µm
b
cm
Qtz
wm
500 µm
c
wm+chl
cm
Qtz+Ab
500 µm
d
cm
Qtz+Chl
500 µm
e
Pl
Ep
Qtz
Grt
Hbl
Ilm
1 mm
f
Ilm
Pl
Grt
Hbl
1 mm
g
wm
Ab
Chl+cb
Ep
Py
Bt
1 mm
h
Chl+wm
cm
Qtz
1 mm

Figure 5

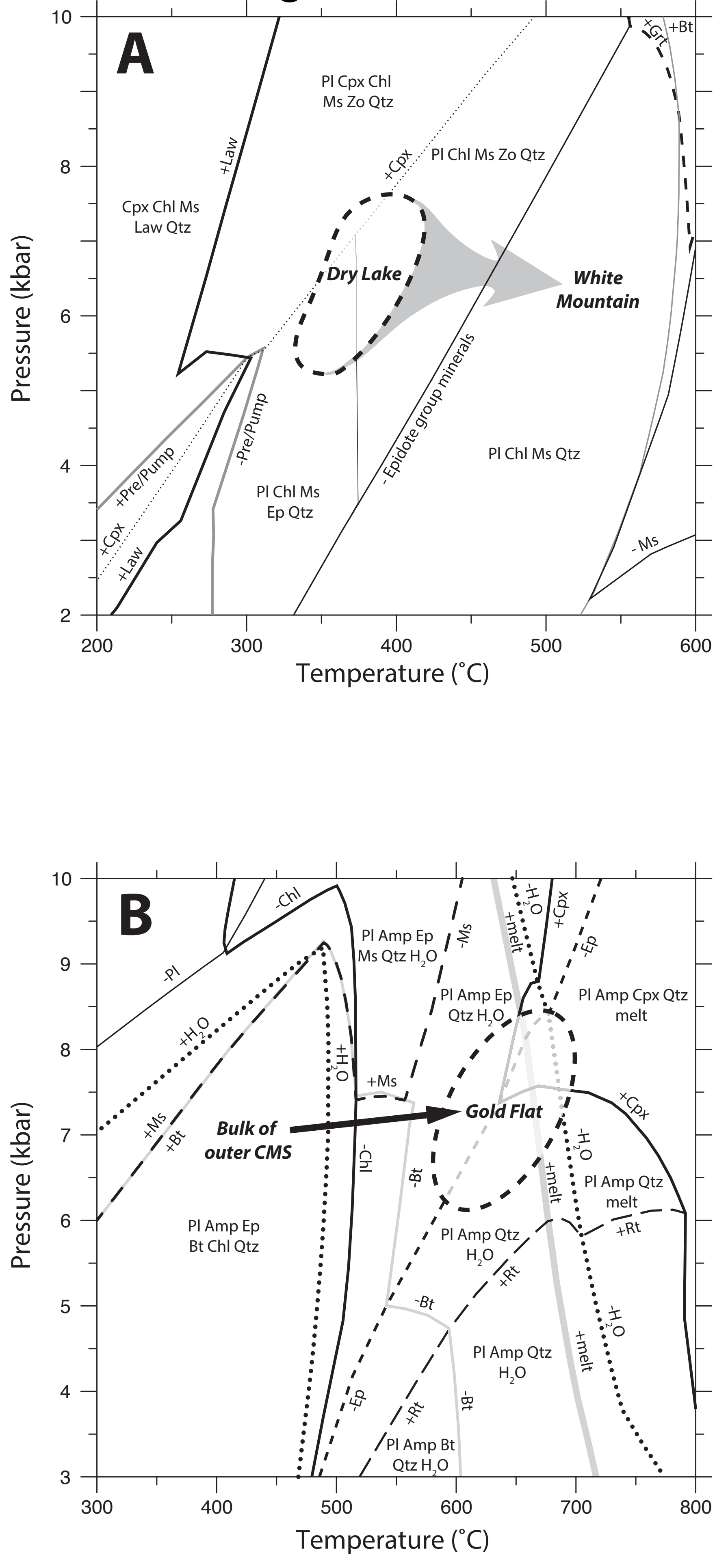
A
Pl Cpx Chl
Ms Zo Qtz
Pl Chl Ms Zo Qtz
Cpx Chl Ms
Law Qtz
+Law
+Cpx
+Grt
+Bt
Dry Lake
White
Mountain
- Epidote group minerals
Pl Chl Ms Qtz
Pl Chl Ms
Ep Qtz
+Pre/Pump
-Pre/Pump
+Cpx
+Law
- Ms
Pressure (kbar)
Temperature (˚C)
B
-Chl
-Pl
Pl Amp Ep
Ms Qtz H2O
-Ms
Pl Amp Ep
Qtz H2O
+melt
+Cpx
-Ep
Pl Amp Cpx Qtz
melt
+Ms
+Bt
+Ms
Bulk of
outer CMS
Gold Flat
-Chl
-Bt
-H2O
+melt
Pl Amp Qtz
melt
+Rt
Pl Amp Ep
Bt Chl Qtz
Pl Amp Qtz
H2O
-Bt
Pl Amp Qtz
H2O
-Ep
+Rt
-Bt
Pl Amp Bt
Qtz H2O
Pressure (kbar)
Temperature (˚C)

Figure 6

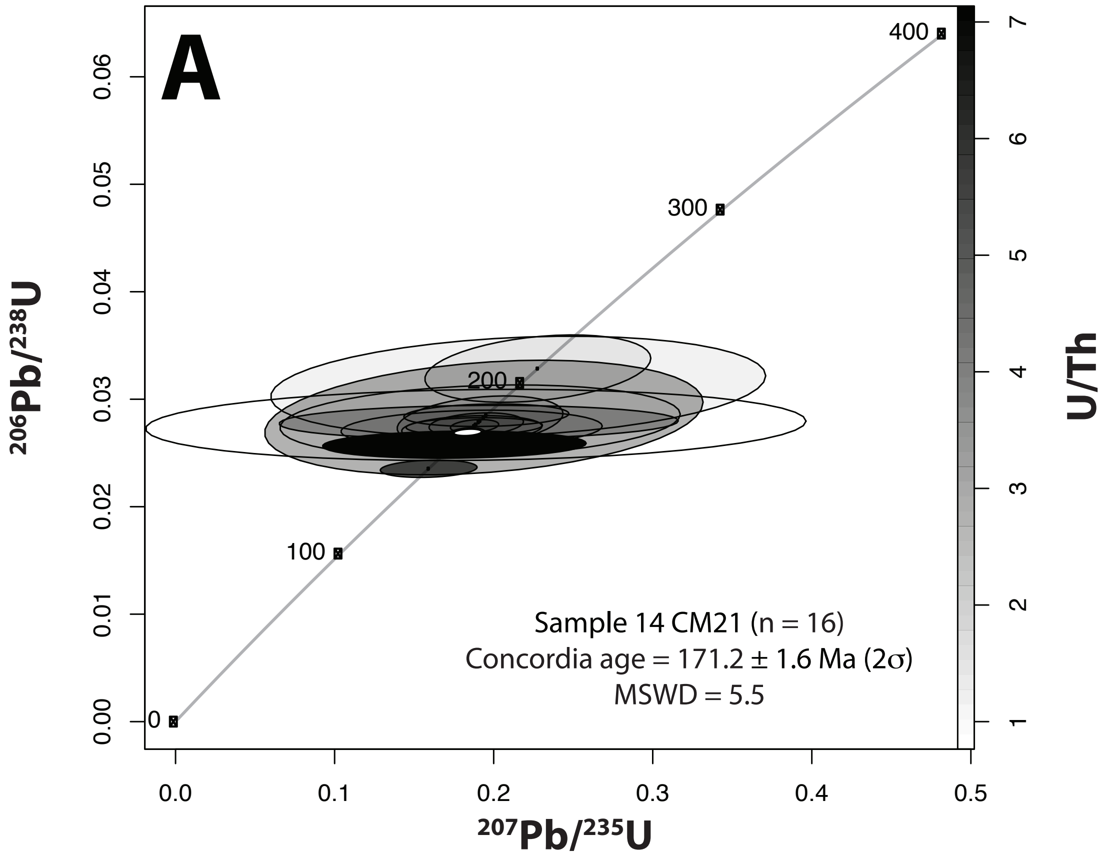

A
0.00
0.01
0.02
0.03
0.04
0.05
0.06
$^{206}Pb/^{238}U$
0.0
0.1
0.2
0.3
0.4
0.5
$^{207}Pb/^{235}U$
0
100
200
300
400
U/Th
1
2
3
4
5
6
7
Sample 14 CM21 (n = 16)
Concordia age = 171.2 ± 1.6 Ma (2σ)
MSWD = 5.5

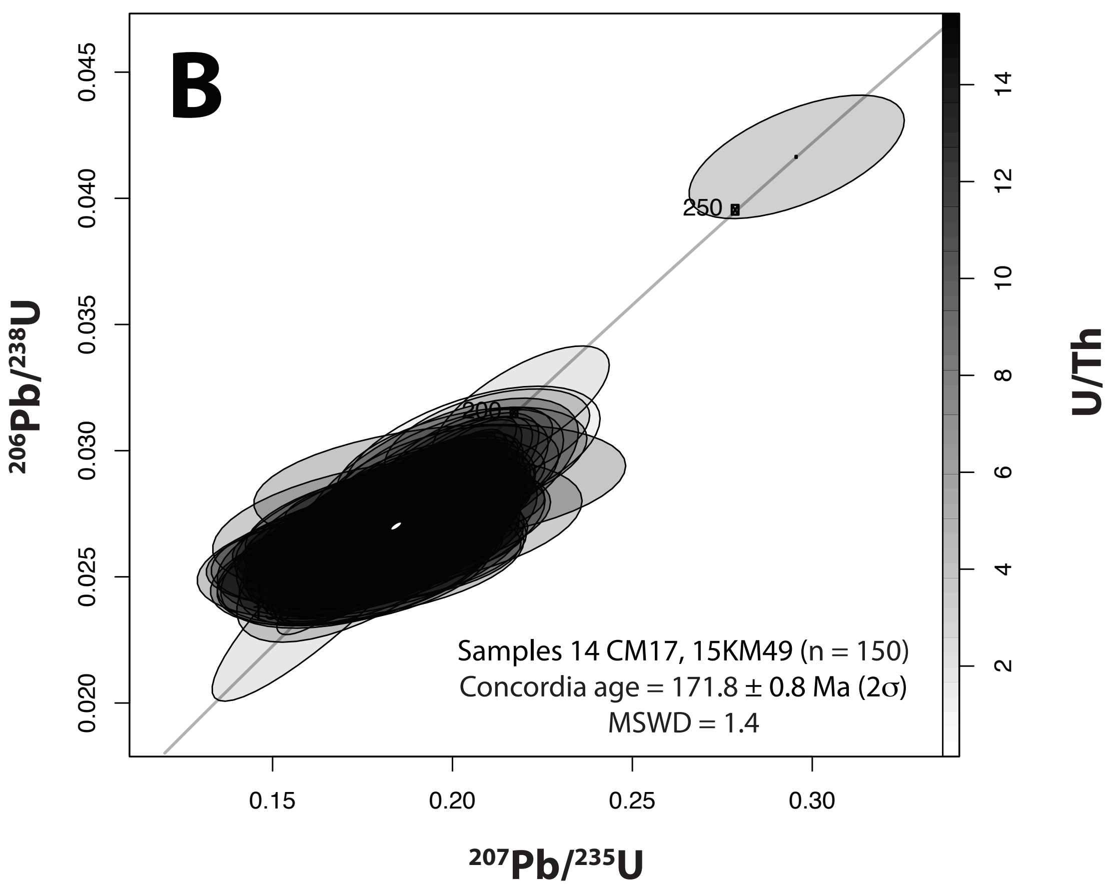

B
0.020
0.025
0.030
0.035
0.040
0.045
$^{206}Pb/^{238}U$
0.15
0.20
0.25
0.30
$^{207}Pb/^{235}U$
200
250
U/Th
2
4
6
8
10
12
14
Samples 14 CM17, 15KM49 (n = 150)
Concordia age = 171.8 ± 0.8 Ma (2σ)
MSWD = 1.4

Figure 7

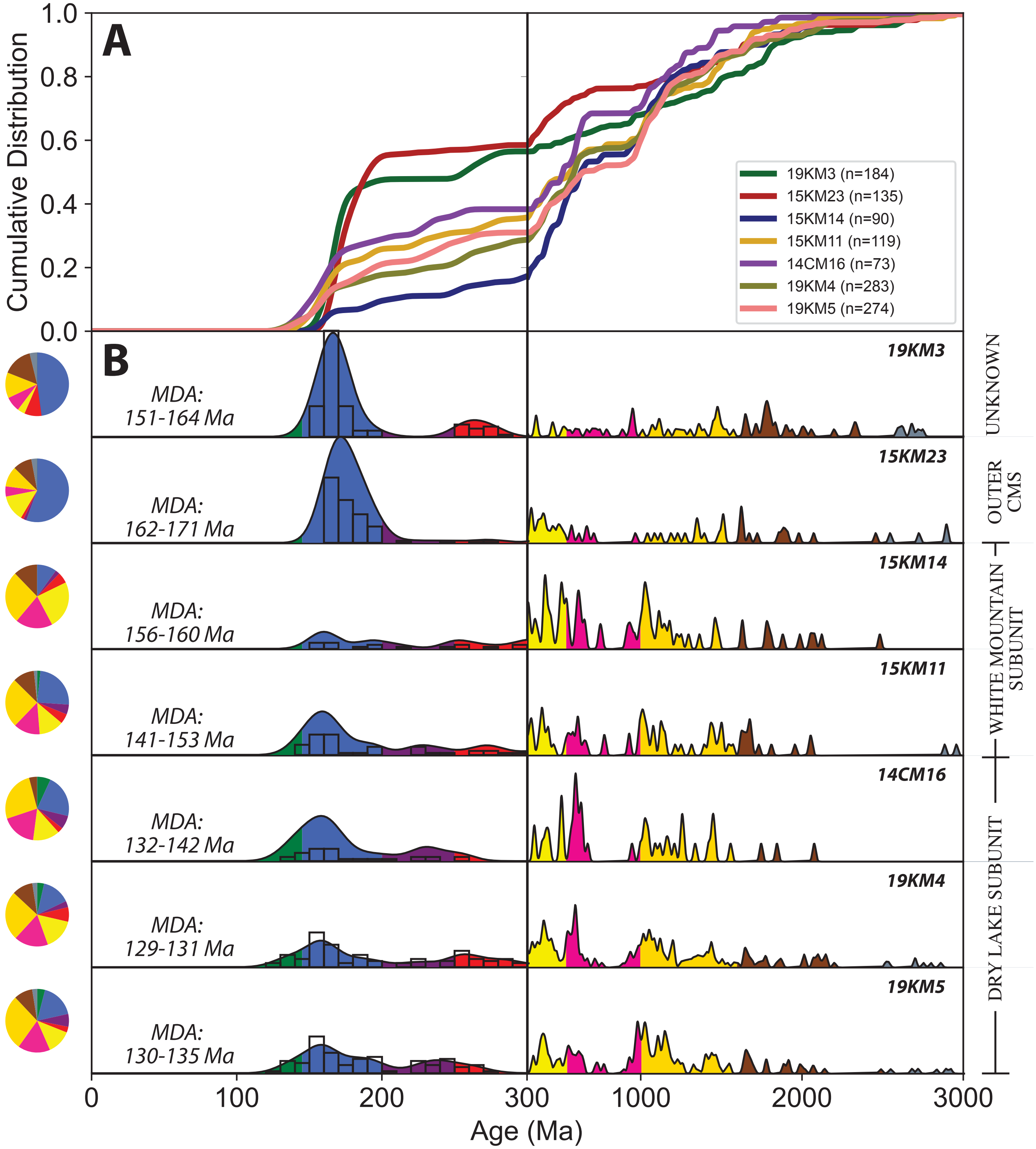

A
B
Cumulative Distribution
1.0
0.8
0.6
0.4
0.2
0.0
19KM3 (n=184)
15KM23 (n=135)
15KM14 (n=90)
15KM11 (n=119)
14CM16 (n=73)
19KM4 (n=283)
19KM5 (n=274)
MDA: 151-164 Ma
19KM3
MDA: 162-171 Ma
15KM23
MDA: 156-160 Ma
15KM14
MDA: 141-153 Ma
15KM11
MDA: 132-142 Ma
14CM16
MDA: 129-131 Ma
19KM4
MDA: 130-135 Ma
19KM5
UNKNOWN
OUTER CMS
WHITE MOUNTAIN SUBUNIT
DRY LAKE SUBUNIT
0
100
200
300
1000
2000
3000
Age (Ma)

Figure 8

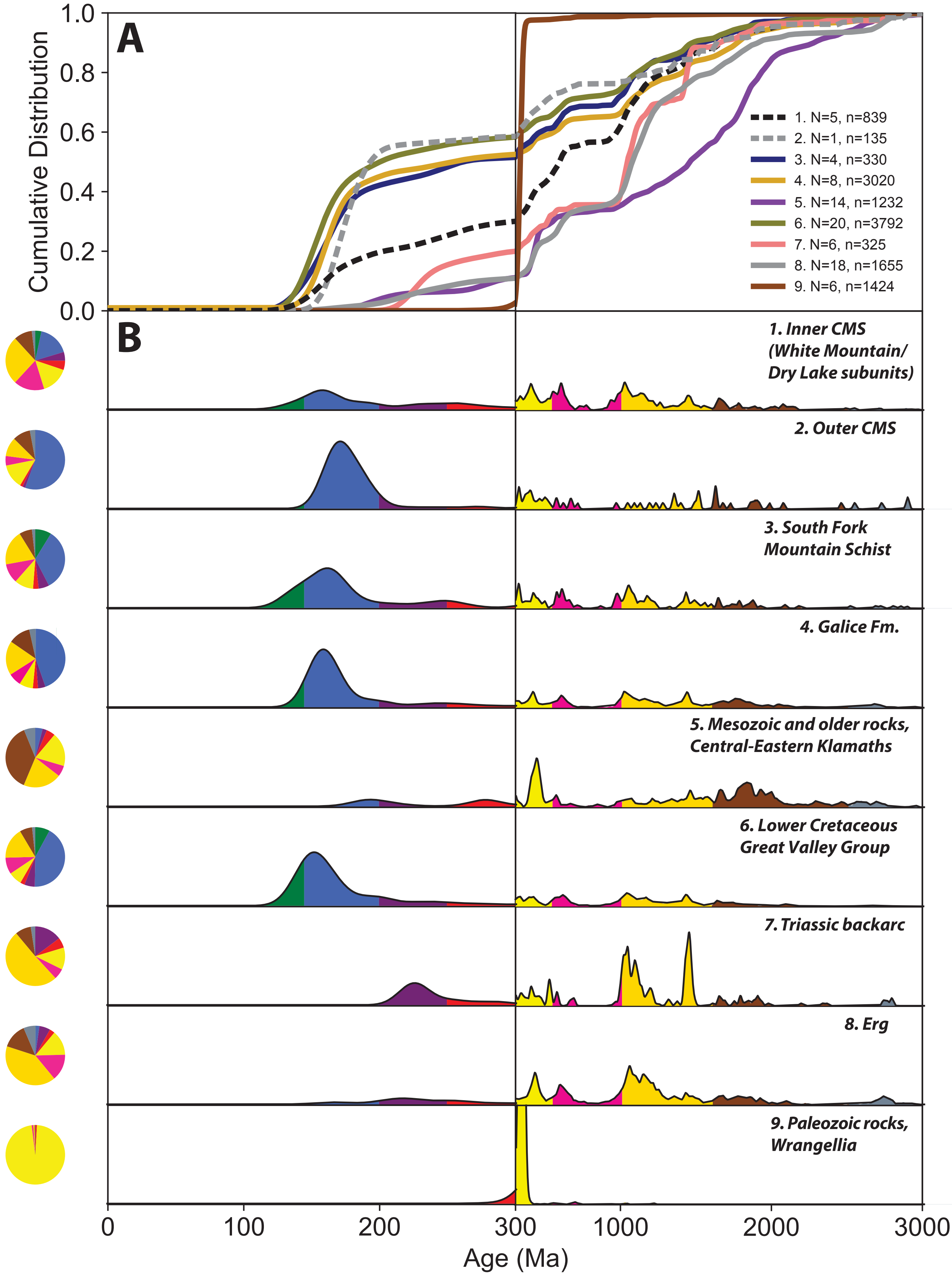

A
B
1.0
0.8
0.6
0.4
0.2
0.0
Cumulative Distribution
1. N=5, n=839
2. N=1, n=135
3. N=4, n=330
4. N=8, n=3020
5. N=14, n=1232
6. N=20, n=3792
7. N=6, n=325
8. N=18, n=1655
9. N=6, n=1424
1. Inner CMS (White Mountain/ Dry Lake subunits)
2. Outer CMS
3. South Fork Mountain Schist
4. Galice Fm.
5. Mesozoic and older rocks, Central-Eastern Klamaths
6. Lower Cretaceous Great Valley Group
7. Triassic backarc
8. Erg
9. Paleozoic rocks, Wrangellia
0
100
200
300
1000
2000
3000
Age (Ma)

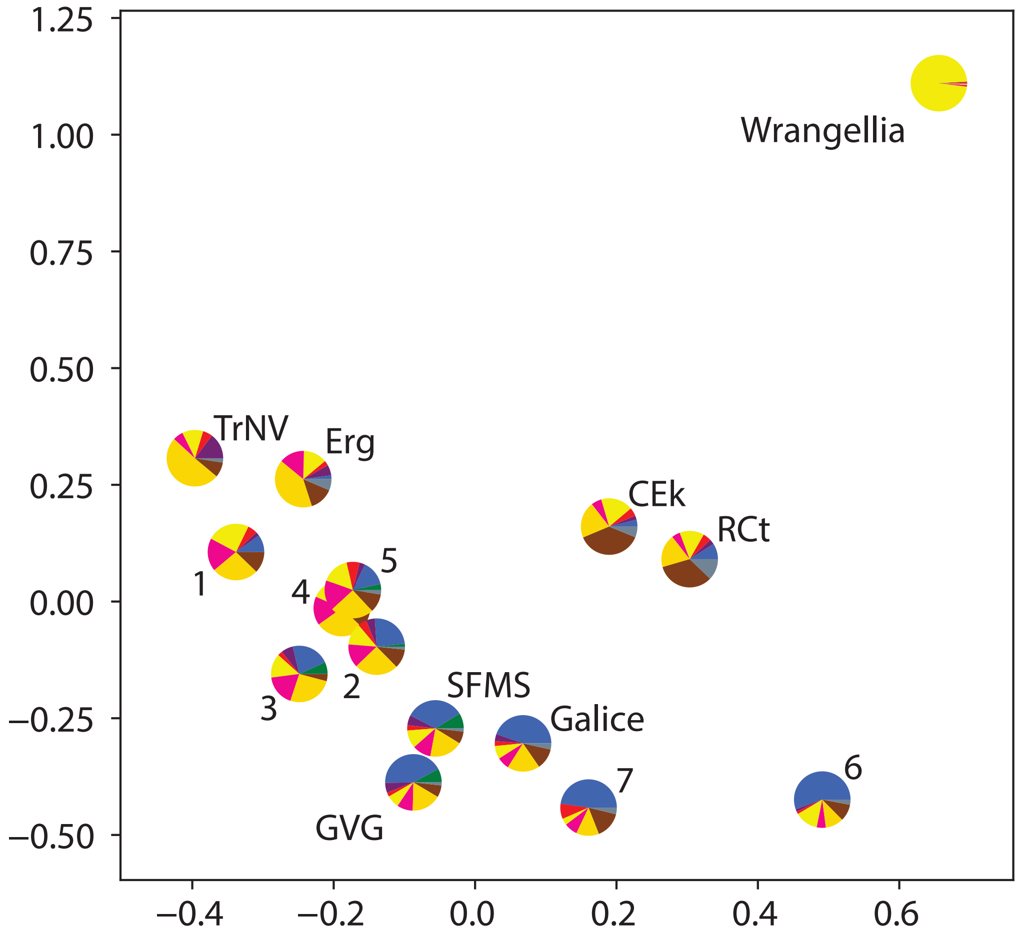

1.25
1.00
0.75
0.50
0.25
0.00
−0.25
−0.50
−0.4
−0.2
0.0
0.2
0.4
0.6
Wrangellia
TrNV
Erg
CEk
RCt
1
2
3
4
5
6
7
SFMS
Galice
GVG

Figure 10

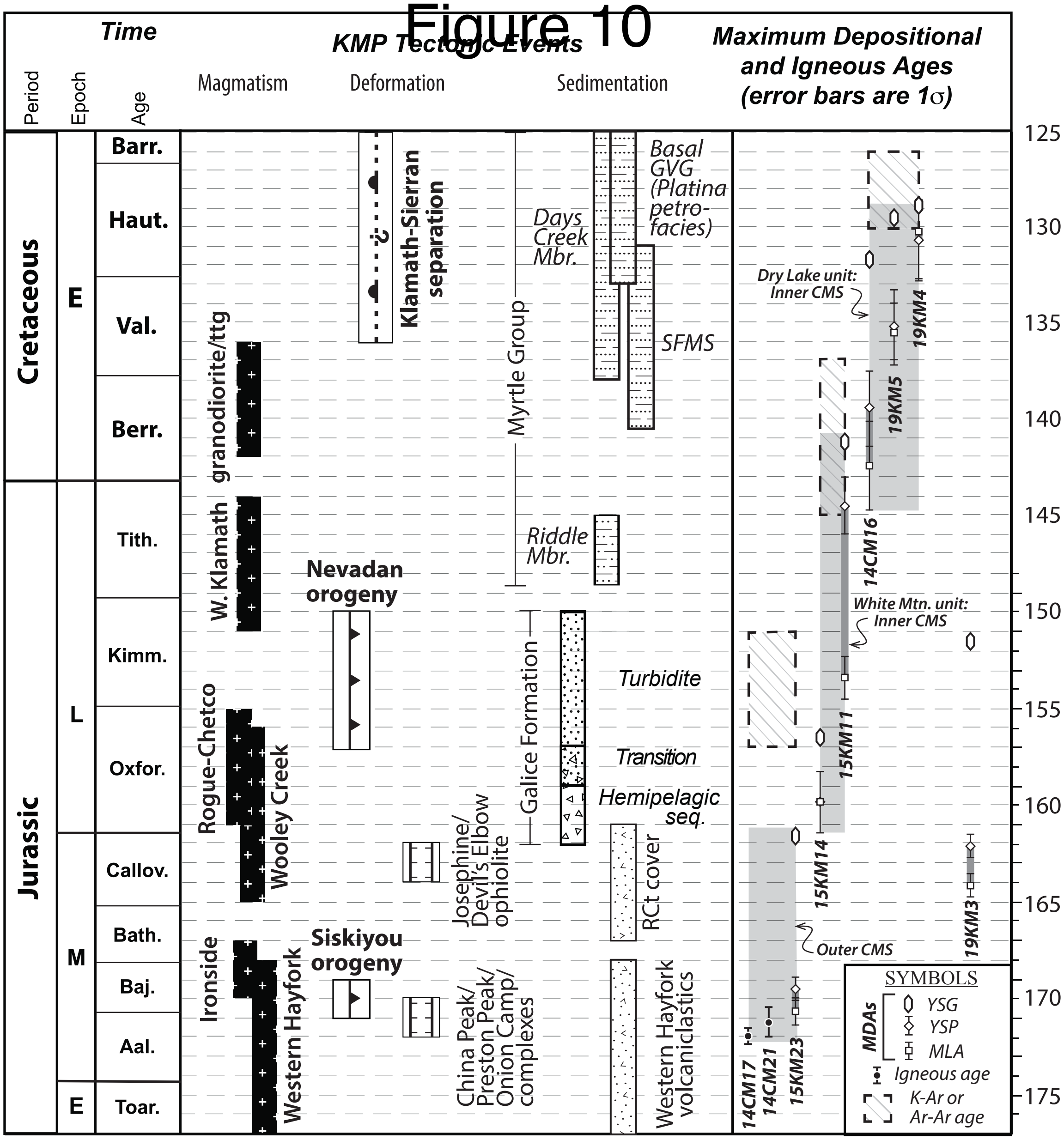
Time
KMP Tectonic Events
Maximum Depositional and Igneous Ages (error bars are 1σ)
Period
Epoch
Age
Magmatism
Deformation
Sedimentation
Cretaceous
Jurassic
E
L
M
E
Barr.
Haut.
Val.
Berr.
Tith.
Kimm.
Oxfor.
Callov.
Bath.
Baj.
Aal.
Toar.
granodiorite/ttg
W. Klamath
Rogue-Chetco
Wooley Creek
Ironside
Western Hayfork
Klamath-Sierran separation
Nevadan orogeny
Siskiyou orogeny
Josephine/ Devil's Elbow ophiolite
China Peak/ Preston Peak/ Onion Camp/ complexes
Myrtle Group
Days Creek Mbr.
Riddle Mbr.
Galice Formation
Basal GVG (Platina petro-facies)
SFMS
Turbidite
Transition
Hemipelagic seq.
RCt cover
Western Hayfork volcaniclastics
Dry Lake unit: Inner CMS
White Mtn. unit: Inner CMS
Outer CMS
19KM4
19KM5
14CM16
15KM11
15KM14
19KM3
14CM17
14CM21
15KM23
SYMBOLS
MDAs
YSG
YSP
MLA
Igneous age
K-Ar or Ar-Ar age
125
130
135
140
145
150
155
160
165
170
175

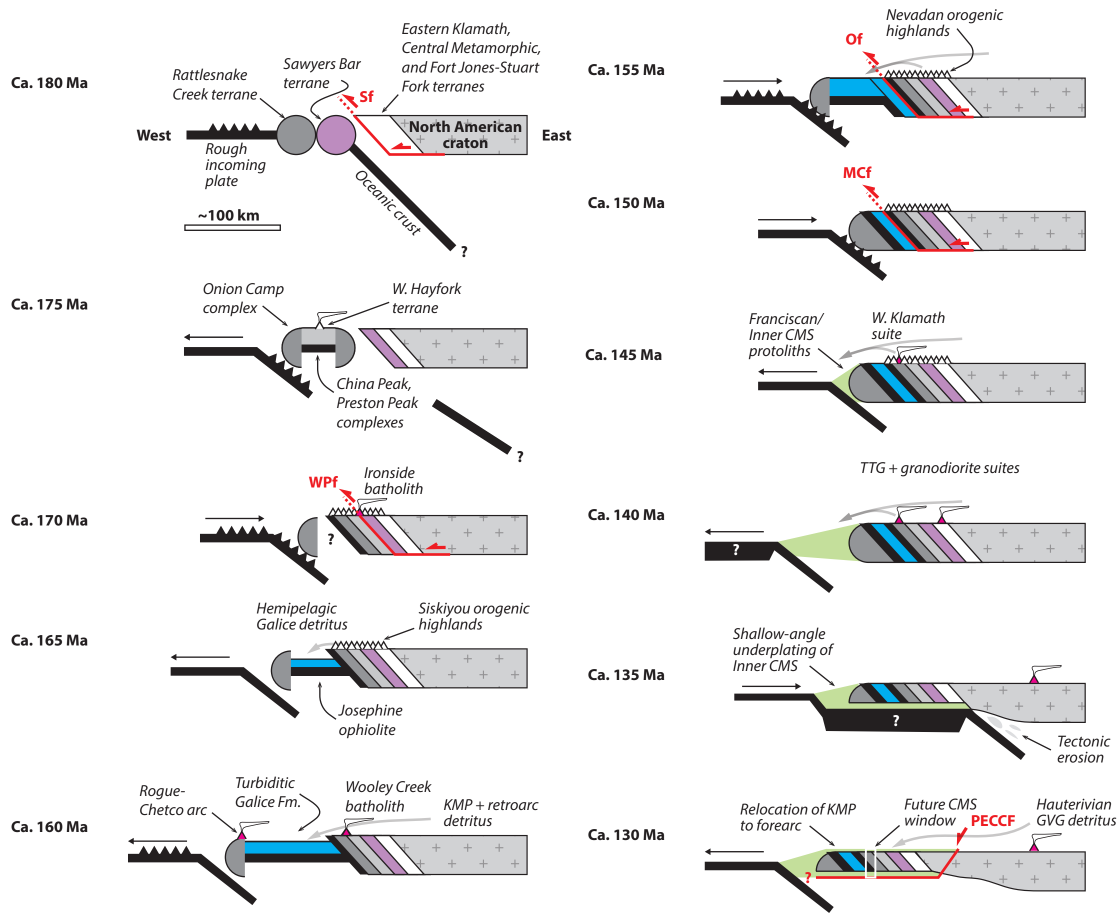

Ca. 180 Ma
Rattlesnake Creek terrane
Sawyers Bar terrane
Sf
Eastern Klamath, Central Metamorphic, and Fort Jones-Stuart Fork terranes
West
North American craton
East
Rough incoming plate
Oceanic crust
~100 km
?
Ca. 175 Ma
Onion Camp complex
W. Hayfork terrane
China Peak, Preston Peak complexes
Ca. 170 Ma
WPf
Ironside batholith
Ca. 165 Ma
Hemipelagic Galice detritus
Siskiyou orogenic highlands
Josephine ophiolite
Ca. 160 Ma
Rogue-Chetco arc
Turbiditic Galice Fm.
Wooley Creek batholith
KMP + retroarc detritus
Ca. 155 Ma
Of
Nevadan orogenic highlands
Ca. 150 Ma
MCf
Ca. 145 Ma
Franciscan/ Inner CMS protoliths
W. Klamath suite
Ca. 140 Ma
TTG + granodiorite suites
Ca. 135 Ma
Shallow-angle underplating of Inner CMS
Tectonic erosion
Ca. 130 Ma
Relocation of KMP to forearc
Future CMS window
PECCF
Hauterivian GVG detritus

TABLE 1. SAMPLE LOCATIONS AND DESCRIPTIONS.

Sample	Abbreviation	Rock Unit	Description	UTM Zone	UTM Easting	UTM Northing
15KM14	1	WM CMS	Graphitic schist	10T	494664	4644493
15KM11	2	WM CMS	Graphitic schist	10T	495747	4637173
14CM16	3	Inner CMS	Graphitic schist	10T	501716	4642816
19KM5	4	Inner CMS	Graphitic schist	10T	503222	4641838
19KM4	5	Inner CMS	Graphitic schist	10T	503868	4641015
15KM23	6	Outer CMS	Semipelite of Helper (1985)	10T	490621	4642545
19KM3	7	Unknown; Outer CMS	Quartzofeldspathic schist	10T	476118	4627262
15KM49/14CM1	8	Outer CMS	Metamorphosed felsic stock	10T	499148	4621960
14CM21	9	Unknown; Outer CMS	Gold Flat amphibolite of Burton (1982)	10T	491966	4614462

TABLE 2. DEPOSITIONAL AGE CONSTRAINTS FOR DETRITAL ROCKS STUDIED HEREIN. SEE TEXT FOR DISCUSSION OF MAXIMUM DEPOSITIONAL AGE CALCULATIONS.

Sample	Abbreviation	Rock Unit	N	YSG (Ma)	YSG 2σ	YSP* (Ma)	2σ	MSWD	MLA* (Ma)	2σ	Most relevant deposition-bracketing age (Ma)	Interpreted depositional age
15KM23	6	Outer CMS	135	161.6	8.4	169.5	1.9	1.0	170.8	*2.0*	156-152†	Middle or Upper Jurassic
15KM14	1	WM CMS	90	156.5	7.9	*159.8*	*3.5*	*0.6*	*159.8*	*3.5*	144§	Upper Jurassic
15KM11	2	WM CMS	119	141.1	5.1	*144.5*	*3.2*	*1.2*	*153.4*	*2.6*	144§	Upper Jurassic or Lower Cretaceous
14CM16	3	Inner CMS	73	131.7	7.8	*139.5*	*4.0*	*1.7*	*142.5*	*5.0*	128#	Lower Cretaceous
19KM5	4	Inner CMS	274	129.5	8.5	*135.1*	*2.1*	*1.0*	*135.5*	*2.3*	128#	Lower Cretaceous
19KM4	5	Inner CMS	283	128.9	2.9	*130.7*	*2.1*	*1.6*	*130.2*	*3.5*	128#	Lower Cretaceous
19KM3	7	Unknown	184	151.4	16.2	162.1	1.6	1.0	164.2	1.6	not available	Upper Jurassic

Note: MSWD—mean square of weighted deviates; N - number of analyzed grains; YSG—youngest single grain; YSP—youngest statistical population (Coutts et al., 2019); MLA—maximum likelihood algorithm (Vermeesch, 2021).

*YSP (Coutts et al., 2019) and MLA (Vermeesch, 2021) uncertainties include both analytical and systematic uncertainties.

† K-Ar and Ar-Ar hornblende (Helper, 1985; Saleeby and Harper, 1993)

§ K-Ar white mica (Lanphere et al., 1968)

K-Ar white mica (Helper)